CHALMERS

Optimal working conditions of a floatel along an FPSO

Master's Thesis in the International Master's Programme Naval Architecture and Ocean Engineering

SETH KUNKYEBE

YORDAN GEORGIEV

Department of Shipping and Marine Technology
Division of Marine Technology
CHALMERS UNIVERSITY OF TECHNOLOGY
Göteborg, Sweden 2015
Master's thesis 2015: X - 15/319

MASTER'S THESIS IN THE INTERNATIONAL MASTER'S PROGRAMME IN NAVAL ARCHITECTURE AND OCEAN ENGINEERING

Optimal working conditions of a floatel along an FPSO

SETH KUNKYEBE

YORDAN GEORGIEV

Department of Shipping and Marine Technology
Division of Marine Technology
CHALMERS UNIVERSITY OF TECHNOLOGY
Göteborg, Sweden 2015

Optimal working conditions of a floatel along an FPSO

SETH KUNKYEBE
YORDAN GEORGIEV

Master's Thesis 2015: X - 15/319 Yordan Georgiev & Seth Kunkyebe
Department of Shipping and Marine Technology
Division of Marine Technology
Chalmers University of Technology
SE-412 96 Göteborg
Sweden
Telephone: + 46 (0)31-772 1000

Cover: Floatel Reliance model. Courtesy of Floatel International AB

Printed by Chalmers Reproservice
Göteborg, Sweden 2015

Optimal working conditions of a floatel along an FPSO

Master's Thesis in the International Master's Programme in Naval Architecture and Ocean Engineering

SETH KUNKYEBE
YORDAN GEORGIEV
Department of Shipping and Marine Technology
Division of Marine
Chalmers University of Technology

ABSTRACT

Offshore operations are normally involving the connection between two or more floating structures. The arrangement, connection framework and connection effects due to encountered weather conditions etc., have been studied by a series of research and development activities. This thesis project aims to determine the optimal connection and operation arrangement with regard to minimum operation power requirement for a floating hotel under different environment conditions.

The floating hotel is a semi-submersible accommodation unit, which should be attached to a turret moored FPSO and provide services to people working on the FPSO. The connection is organized by a strike gangway. However, the gangway connection is too weak to carry any loads, as it is meant for the transfer of people, tools, etc. between the two. The only way for this specific set up to work is if the accommodation unit follows the motions of the FPSO with the aid of a DP system, while fulfilling two specific conditions.

Firstly, the gangway length has a tolerance of only +/-3 meters. In case elongation beyond or shortening under that limit occurs, an alarm is set off and the vessels should be detached. It is essential that the deformation of the gangway doesn't exceed +/-5 meters at any time, as this would damage either the telescopic part of it or the connecting mechanism.

Secondly, the gangway inclination also has limits. If it reaches 3 degrees on either side, the connection should be interrupted. This condition isn't dependent on the DP system as much as on the sea-keeping, but it is the reason for the limiting sea states.

A number of simulations are done in order to investigate three different orientations between the vessels (parallel, diagonal and perpendicular) under various environmental conditions. In the end of the thesis, the results are compared in order to choose a preferable/optimal relative angle for the gangway connection and specific occurrences during the simulations are discussed.

Keywords: Accommodation unit; connection; FPSO; gangway; SIMO; thrust force

Content

Preface

This thesis is a part of the requirements for the master's degree in Naval Architecture and Ocean Engineering at Chalmers University of Technology, Göteborg, and has been carried out at the Division of Marine Design, Department of Shipping and Marine Technology, Chalmers University of Technology between January and June of 2015.

We would like to acknowledge and thank our examiner and academic supervisor, Associate Professor Wengang Mao, and our company supervisor Yungang Liu, at Floatel International AB, for their tremendous guidance and support throughout the work with this thesis.

Göteborg, May 2015

Seth Kunkyebe

Yordan Georgiev

1 Introduction

1.1 Background

In the last decade there has been a depletion of easily accessible offshore oil. The demand for crude oil however continues to rise as many industries continue to depend on oil and gas as a source of energy for their production. In order to meet the growing demand for offshore oil and gas, oil and gas production companies are forced to explore deeper waters many miles away from land. The increase in prices have made it feasible for companies to invest in high end and advanced technologies that will be able to be used in the new environment.

The remote location of the deep water oil exploration means that personnel working on board the oil rigs have to be accommodated offshore. As a solution to this, a purposely built accommodation platform is employed to house the rig personnel during their working period offshore. The platform is designed and constructed to meet a standard that is considered safe for the inhabitants. It consists of all the essential necessities that are required for basic human lodging. This does not mean that some accommodation platforms do not go further to provide a luxurious way of living comparable to a hotel on land. The purpose built accommodation platform colloquially called "floatel" was built at the Götaverken Cityvarvet shipyard in Gothenburg, Sweden in 1977 (JCE Group of Companies, 2015).

Floatel International Limited located in Mölndal, Sweden has been in the offshore accommodation market since 2006. They provide offshore accommodation units to the oil and gas industry worldwide. The company's seeks to provide the most state-of-the-art, safe and reliable offshore accommodation in order to meet the rising demand in the offshore accommodation market (Floatel International Ltd, 2015).

The first floatel named Floatel Superior was delivered in March 2010. It has an accommodation size of 440 or 512 beds depending on single or double occupancy. The second is Floatel Reliance, it has 500 bed accommodations. There are in total four Floatels currently in operation. The last of which was delivered in April 2015. All Floatels are equipped with dynamic positioning (DP) capabilities. This ensures that they keep their position in connecting their gangway to the vessel.

This thesis focuses on the station keeping ability of Floatel Reliance which is to carry out an assignment for Petrobras in Brazil. For the purpose of this report the Floatel Reliance will only be referred to as 'floatel'. The operation of the floatel is such that, operation time is counted only when the gangway of the floatel is connected to the supporting vessel in order to allow personnel to transfer to the work platform to the accommodation platform. For this reason, floatel needs to ensure that it is able to follow the target vessel within a given displacement range allowable by the telescopic action of its gangway. As a result the economic value of the floatel depends mostly on the performance of the DP system. To achieve the maximum revenue from the DP system must work effectively and with maximum efficiency.

1.2 Objectives

The current investigation is carried out for the Floatel Reliance. The main objective of this study is to determine the optimal operational conditions of the Floatel in connection with a FPSO. The study mainly focuses on the determination of thruster force allocation that will be needed for the DP performance under different environmental conditions. During operation of the vessel, power generated on board is predominantly used to support accommodation necessities and power the propulsion of the four thrusters for dynamic positioning. In this regard, the reduction of power required by the thrusters for DP operation can cut down the costs of operation. It also important to note that the revenue for the service of the floatel is calculated with regard to the time in which the gangway of the floatel remains connected to the FPSO. It is consequently very important for the DP system of the floatel to be able to keep a fixed position relative to the moving FPSO.

Another part of the study is focused on the best orientation of the floatel when the gangway is connected to the FPSO. The various orientations are illustrated in Figure 1.1. Three different orientations are proposed by Floatel International AB. The orientation is important because it changes the alignment of the pontoons with respect to the direction of the ocean current. The turret mooring system of the FPSO ensures that the FPSO positions itself at an advantageous orientation towards the heading of the strongest environmental force. For the FPSO, the current forces are ascertained as the dominant force.

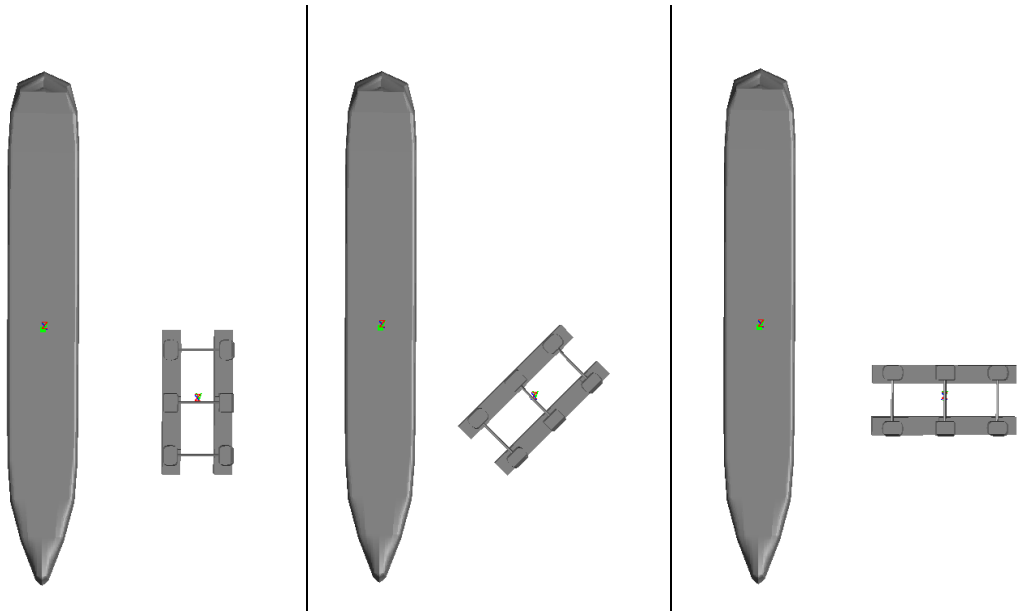

Figure 1.1 Proposed orientations of semi-submersible floatel relative to a FPSO: parallel, diagonal and perpendicular.

The study will be carried out in different environmental scenarios to get a broad data to base the findings on and to give an elaborate analysis. All the weather data used in the study is taken from the environmental conditions and motions from oil fields operation manual of the operation location of the vessel

To sum it up, the overall objective is to investigate the best orientation of the semi-submersible floatel that will require less thruster utilization with regard to follow target.

In order to achieve such an objective, the following tasks will be carried out during the thesis:

- Determine and simulate the individual cases of environmental conditions to carry out the simulation, with each case being a combination of conditions for current, waves and wind.

- Study the vessel motions in each of the simulations.

- Tune the DP control parameters to obtain the best possible performance that is to maintain a small footprint as well as consuming less thruster power.

- Account for the boundary condition of the gangway that will incorporate the +/-3 metres stroke.

A total of 36 simulations are done to obtain time series of the motion response for the FPSO. There are 108 additional simulations to find the best orientation and the impact of DP controller parameters on the follow target ability of the floatel.

1.3 Methodology

In order to attain the wave induced motion responses of the two vessels, a comprehensive knowledge of the sea environment (wind, wave and current), vessel hydrodynamics and mooring systems is required. In this thesis project, the DNV sesam package DeepC (Det Norske Veritas, 2013) will be used to perform the above mentioned analysis.

The DeepC software comprises two modules, Simo and Riflex. The two modules perform the nonlinear time domain analysis in two steps:

1. **Static equilibrium analysis:** This analysis starts with the configuration of the lines without any stresses acting on them. The static analysis calculates for a number of static load steps and gives a result of the line ends in specified static position of support points and also the static vessel position due to the influence of the connecting lines (Det Norske Veritas, 2013).

2. **Dynamic analysis:** This analysis starts with the static equilibrium positions and performs a time domain solution of the system (vessel with connecting lines) exposed to all its different loads.

The simulation procedure in DeepC is visualized in Figure 1.2. The next simulation done with the SIMO program uses the time series of the FPSO as a prescribed displacement. The same environment used in the DeepC simulation is also used. Furthermore, the thruster configuration and DP control parameters are added as additional inputs.

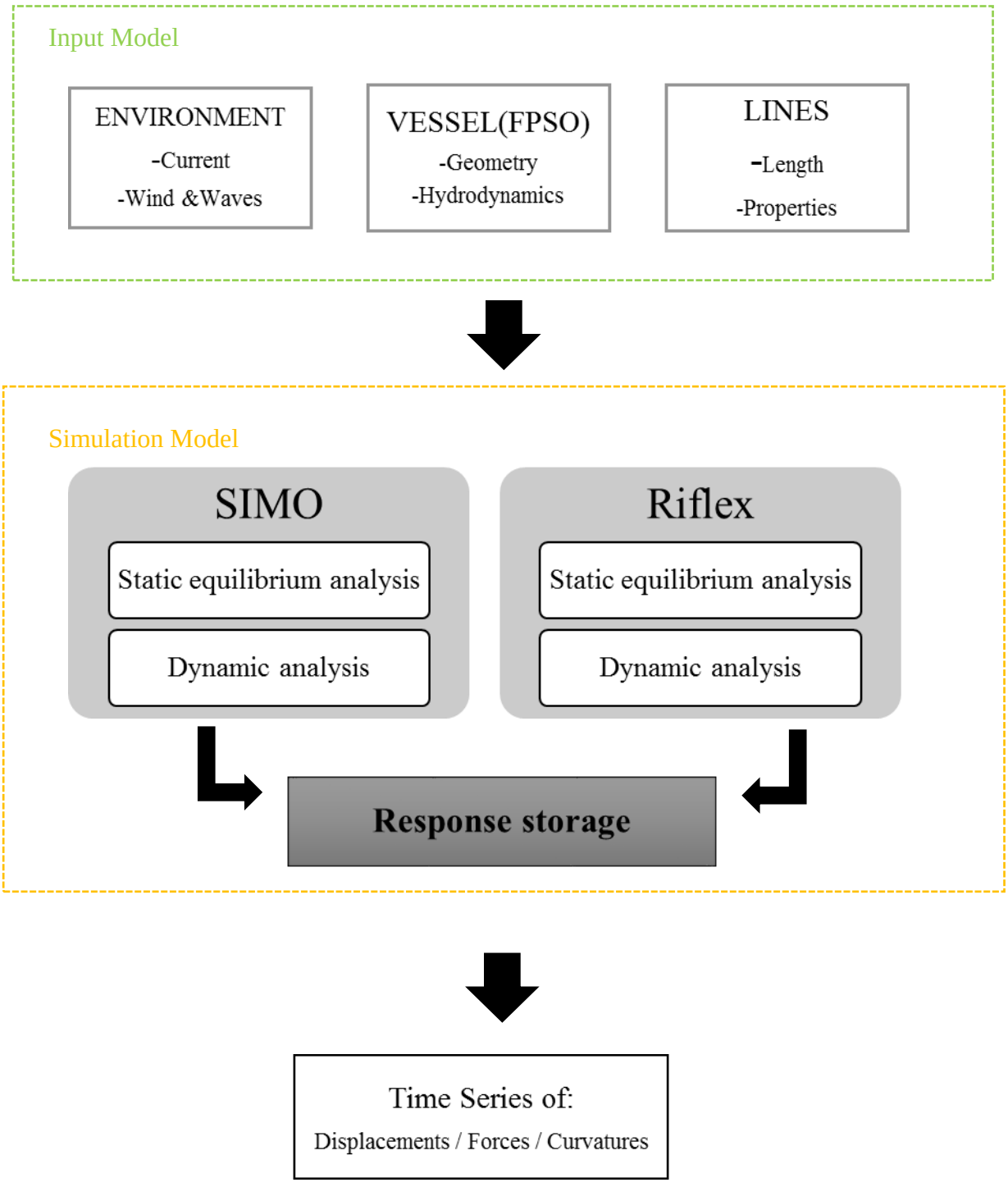

Figure 1.2 Flowchart visualizing the simulation process in DeepC

1.4 Outline of thesis

This thesis has been split into a number of tasks depending on their relevance to the thesis. First, there is an overview of dynamic positioning system and how it is applied in the floatel studied under this thesis. Then the simulation models are further explained in detail to get a clear understanding of their characteristics and hydrodynamic properties.

The location for the study and the weather environment is described in the subsequent chapter. In this chapter, various combinations of magnitudes a direction for current, wind and wave is explained.

Finally, the simulation results of the simulations are presented followed by a discussion on the findings.

1.5 Limitations

There are specific requirements for the layout of the turret mooring system given by the American Petroleum Institute (API) due to the limited time; the same configuration used in the DeepC software was used.

The model for the Petrobras FPSO was made with a summary of the information given by ABS public records. Therefore details of tank plans and compartments were not included to make a full stability analysis. Also, due to the inaccessibility of the wind, current and wave coefficients of the FPSO, the same values for the DNV DeepC example file were used.

The FPSO is also studied under the same loading condition which is with full load in all the simulations.

2 Theory

In this chapter evaluation of the vessel motions is explained. All the theories and equations are taken from the SIMO theory manual (Marintek, 2012a). The vessels in this thesis are to be positioned in a particular location of water so no manoeuvring motions are involved. This chapter describes in detail the theories and assumptions used for the calculations.

A vessel floating on water has 6 degrees of freedom (6 DOF) as displayed in Figure 2.1. They are surge, sway, heave for the translational displacements, as well as roll, pitch, and yaw for the rotational displacements. The heave, roll and pitch motions which are assumed to be as a result of the disturbances of the free-surface is termed the sea-keeping problem.

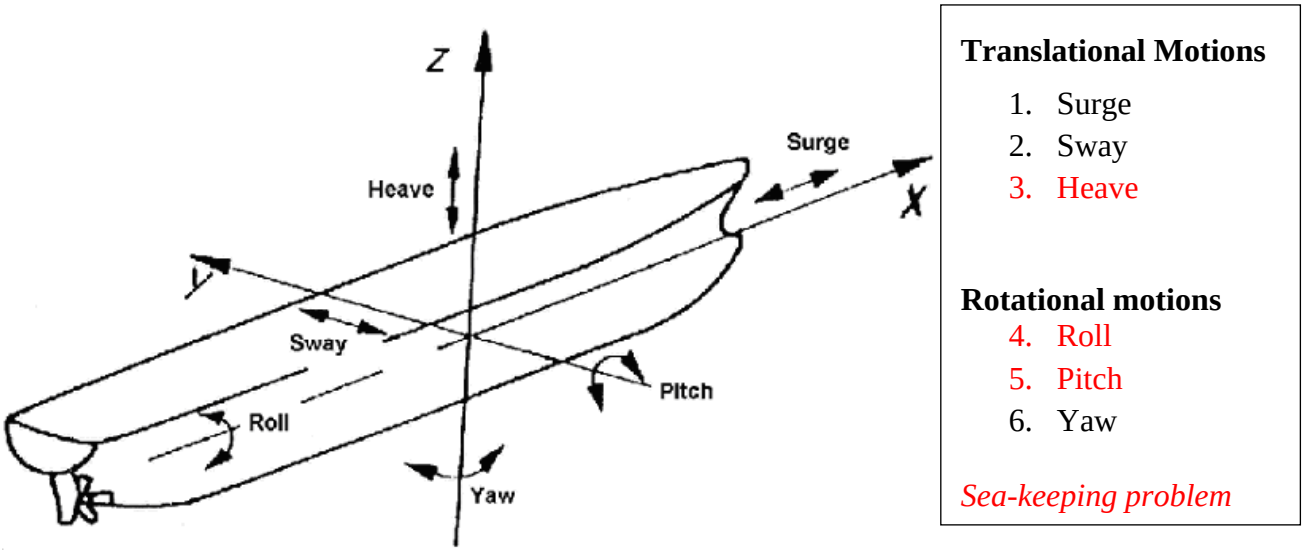

Figure 2.1 Vessels 6 degrees of freedom (Schiffahrtsinsttitut Warnemunde e.V., 2015)

The sea-keeping problem can be expressed if the viscosity of the water is ignored and the water is assumed to be incompressible and irrotational. Irrotational flow is a flow where water lines move in parallel to each other i.e. the do not curl or rotate about their centre.

These assumptions are very helpful in solving the sea-keeping problem numerically and can provide accurate results to determine the motions of a vessel floating in water (Schreuder, 2014).

The numerical analyses of the vessel motions in this thesis are done with the DNVGL software DeepC which uses the SIMO and Reflex programs as their computation solvers. The SIMO program is used for the simulation of sea keeping performance of floating bodies as well as bodies connected to it. The results are presented as time series and statistics of forces and motions of all the bodies and components in the analysed system.

The whole chapter is based on the theory presented by Marintek (2012a). To make it complete, a brief description of the implemented theory is given as follows.

2.1 Coordinate systems

SIMO applies the right-handed Cartesian coordinate systems where the where they are in the rotations are direction as shown in Figure 2.2. The position of all (body) systems are referenced in the global earth-fixed coordinate system. The XY-plane lies on the undisturbed calm water plane. The Z-axis is positive upwards.

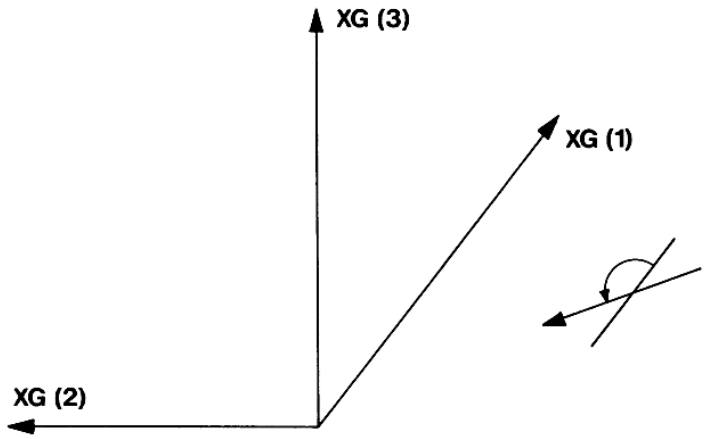

Figure 2.2 Global coordinate system, XG (Marintek, 2012a)

The local coordinate system tracks the body motions. It is defines the coordinates of body parts such as positioning elements and coupling elements. The body-related coordinate system (XB) see Figure 2.3 is the local coordinate system that tracks the horizontal motions of the floating body.

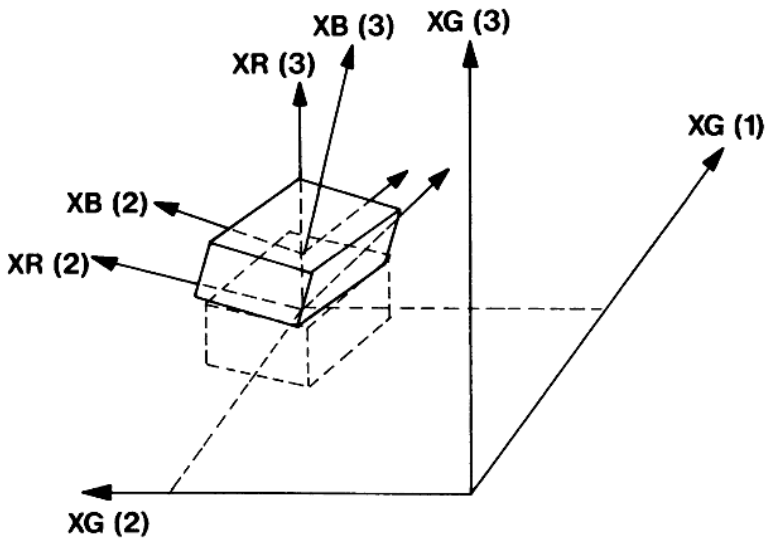

Figure 2.3 Body-related, body-fixed and global coordinate system (Marintek, 2012a)

It is key to define an initial coordinate system. This coordinate system is the original body-related coordinate system of the time domain simulation. The coordinates in this coordinate

system is unchanged throughout the entire simulation. The first-order wave forces and wave drift forces are originated from this coordinate system.

2.2 Generation of time series

As mentioned in the earlier chapter, the aim of this study is to analyse a system and present results for a simulation setup that is non-linear and has a transient character.

In this section, different methods of generating samples of different Gaussian stochastic processes from known mean values and spectra. The spectra are as follows:

- Wind gust.
- Wave elevation and wave particle motions
- First order wave responses
- Second order wave responses

These time series used in this thesis are generated by SIMO by superposition a group of harmonic elements of the simulated environment. The phase of the harmonic elements must have an even distribution. This achieved by pre-generating the elements using the Fast Fourier transform (FFT) (Marintek, 2012a).

2.2.1 Superposition of simulated elements

To generate the time series, the spectrum of the variance of the group of harmonic components is divided to make a number of harmonic elements. After that, the various phases of the harmonic elements are sampled over an even distribution. The phases are distributed over a phase of 0 to 2π.

The time series for a sample is written as:

$$x(t) = \sum_{k=1}^{N} x_k \cos(wt + \phi_k) \tag{2.1}$$

Where, ϕ_k is the sampled phase angle.

All the processes that are linear transformations of $x(t)$ are expressed as:

$$y(t) = \sum_{k=1}^{N} \frac{y_k}{x_k} x_k \cos(wt + \phi_k + \phi_y) \tag{2.2}$$

Where, $\frac{y_k}{x_k}$ is the RAO and ϕ_y is the phase angle or forward phase shift.

Time series generated in this way will have a repetition with a period $T_p = 2\pi/\Delta w_{kmin}$ where w_{kmin} is the smallest increment of the frequency. The random numbers used for phase sampling are generated by reversing a trimmed left root square. The numbers are generated in an almost random manner within a specified interval. They have similar characteristics as random numbers but are not actual randomly generated numbers.

2.2.1.1 Superposition by Fast Fourier transform (FFT)

The most common way to combine several harmonic elements in order to generate a time series is by the Fast Fourier transform (FFT) method. The FFT method must have equal spacing for the frequency. The total sum of frequencies (or number of time samples) is governed by the relation, $N=2^r$ with r being an integer.

The FFT in the SIMO is done using a Cooley-Tukey algorithm. The time increment, Δt, the number of time steps Nt, frequency components, N_w^+ and the frequency increment is expressed as:

$$\Delta_w = \frac{2\pi}{N_t \Delta_t} \qquad (2.3)$$

$$N_w^+ = \frac{N_t}{2+1} \qquad (2.4)$$

From this relation, the duration of the time series for a time increment and the number of steps is limited to:

$$T_p = N_t \Delta_t = \frac{2\pi}{\Delta_w} \qquad (2.5)$$

When the FFT algorithm is used, the positions and vessel headings are first defined before the time series responses are calculated. By this way, the FFT is very efficient and its performance is fully utilized because there is no need to transform the positions and headings. For this reason, short time periods cannot be used for the calculation and then transforming the position. In this case, different strategies are used:

- Each harmonic element is calculated at a defined position with a particular time step and their time-domain functions are added together.
- The FFT is used to calculate the time series for a range of positions and directions and then interpolated to get results of the defined position and time step.

2.2.1.2 By adding of harmonic elements in the time domain

Another method calculating wave responses for each time step in the simulation is by summation of harmonic elements. The results shows the instantaneous locations of each body. This method normally provides a more accurate result for each body, even if there are the coordinates of its position changes. This method takes up more processing time than for an FFT pre-generation, especially for time series with a long duration.

As a result, the pre-generated time series is used together with the cosine series in the time domain to make the process faster. When these two methods are used together, the same result of wave components is used the two methods.

The time series of a sum of harmonic elements has a period of $T_p = 2\pi/\Delta w_{kmin}$. Therefore to avoid a repetition in the wave response, the number of wave components defined in the computation must be high for the extended duration of the computation.

2.2.2 Wind sampling

Wind gusts occurring in the average of the measured wind are simulated by using either the FFT method or by a state-space method made by white noise. The FFT allows the periodic wind gusts to be added to the time series at a quasi-random position.

After generating the wind gust for a particular position, other wind gust at a different positions can created by correlating it to a similar series or generating a non-correlated one using a random independent time series at each position.

2.2.3 Sampling of Waves

The directionality of waves makes its harmonic components slightly different from the harmonic components of wind.

The wave elevation spectra is expressed as:

$$S_\zeta(\beta, \omega) = \theta(\beta)\, S\zeta(\omega) \qquad (2.6)$$

Then the surface elevation is expressed as a function of position dependent phase angle, $\phi p_{jk}$and random phase angle, $\phi\zeta_{jk}$ and given as:

$$\zeta(t) = \sum_{j=1}^{N\beta} \sum_{k=1}^{N\omega} Re\ \tilde{\zeta}_{j,k} e^{i\omega kt} \qquad (2.7)$$

For the harmonic components of the velocity and acceleration of water particles and 1st order responses, they can be obtained as a product of the wave elevation complex transfer functions and its corresponding harmonic component.

2.3 Equations of motion for a vessel

In hydrodynamics, a floating body can be considered as rigid but in motion. By this way, it can exhibit the 6 degrees of freedom. The equations of motion for a vessel is normally given in a body fixed coordinate system ($\bar{x}$, $\bar{y}, \bar{z}$). The vessel motion relative to the earth fixed coordinate system is too large because the forces, moments, moments of inertia and the products of inertia are time dependent. This makes them difficult to calculate. The alternative is to use the body fixed coordinate system where the moments of inertia and the products of inertia are constant to avoid difficulties (Janson, 2014).

Representatively, the equation of motion for a rigid body can simply be expressed as:

$$\underline{F} = M\underline{\ddot{\eta}} \qquad (2.8)$$

Where:

$\boldsymbol{M}$- Mass matrix

$\underline{\ddot{\eta}}$- The body's acceleration for $\underline{\eta} = [\eta_1 \eta_2 \eta_3 \eta_4 \eta_5 \eta_6]^T$ vector of positions in 6 DOF

$\underline{F}$ – Vector of forces and moments acting on the body

$$\underline{F} = (Fx\ Fy\ Fz\ Mx\ My\ Mz) = (F_1 F_2 F_3 F_4 F_5 F_6) \qquad (2.9)$$

The sea keeping problem is described by $F_3, F_4\ and\ F_5$ for the heave, roll and pitch motions respectively.

The results from solving the equations of motion in the body fixed coordinate system, provides information of the motions of the origin of the system and the orientation about the axes. Motions of the vessel are determined by comparing the orientation in the body fixed coordinate system to the global or earth fixed coordinate system. The origin is normally located at the centre of gravity or on the still water surface above the centre of buoyancy.

2.3.1 Kinetics of floating rigid body

$$\dot{\boldsymbol{P}}_b = \boldsymbol{F} \qquad (2.10)$$

$$\dot{\boldsymbol{L}}_b = \boldsymbol{M} \qquad (2.11)$$

Where:

$\dot{\boldsymbol{P}}_b$- Linear momentum

$\boldsymbol{L_b}$ - angular momentum about a point

$\boldsymbol{F}$ - External force

$\boldsymbol{M}$ - External moment a reference point

For $\boldsymbol{L_b}$ and $\boldsymbol{M}$, the origin of the body-fixed coordinate system i.e. (0,0) is used as the reference point.

The linear momentum and angular momentum about the origin are expressed by the relation:

$$P_b = m(v + \omega * r_c) \quad (2.12)$$

$$L_b = I\omega + mr_c * v \quad (2.13)$$

Where:

$\boldsymbol{m}$ – Mass of the floating body

$\boldsymbol{v}$ - Velocity with which the body is moving, measured at the origin

$\boldsymbol{\omega}$- Angular velocity of the floating body with the origin as reference

$\boldsymbol{r_c}$ – Centroid of the floating body in relation to the body origin

$\boldsymbol{I}$ - Inertia tensor of the body in relation to the body origin

The time derivatives for the external force and external moment in the body-fixed coordinate system is written as:

$$F = P'_b + \omega * P_b \quad (2.14)$$

$$M = L'_b + \omega * L_b + v * P_b \quad (2.15)$$

Here, $\boldsymbol{\omega}$ in the above equations is due to the rotating body of reference. The $\boldsymbol{L_b}$ in the second equation is due to the translational motion of the body origin.

2.3.2 Solving of equations of motion by time integration in DeepC

The sea keeping problem can be solved by numerical methods for viscous flow including free surface potential and a model with 6 DOF for the ship motions. Three methods for numerical integration are available in the DeepC software. They are:

1. Improved Euler method
2. Third order method similar to the Runge-Kutta method
3. Newmark-β predictor-corrector method

The Newmark-β predictor-corrector method is used in the simulations used for the simulations in this thesis. The method uses an algorithm that progresses in two steps. The first one is the predictor equation that calculates a rough approximation of the desired response. The second is the corrector equation that filters the initial response to give a more accurate result.

Predictor equation:

$$x_{k+1}^{(0)} = \dot{x}_k + Tf_k \quad (2.16)$$

$$x_{k+1}^{(0)} = x_k + T\dot{x}f_k^{(0)} \quad (2.17)$$

Where, T denotes the step size.

Corrector equation:

$$f_{k+1}^{(i)} = f(x_{k+1}^{(i)}, \dot{x}_{k+1}^{(i)}, \xi_{k+1}^{(i)}) \quad (2.18)$$

$$\dot{x}_{k+1}^{(i+1)} = \dot{x_k} + T(1-\gamma)f_k + \gamma f_{k+1}^i \quad (2.2.19)$$

$$\dot{x}_{k+1}^{(i+1)} = x_k + T\dot{x}_k + \left(\frac{1}{2} - \beta\right)T^2 f_k + \beta T^2 f_{k+1}^i \quad (2.20)$$

The corrector equations are used over and over again for a given number of repetitions until the following condition is achieved:

$$\left|x_{k+1}^{(i+1)} - x_{k+1}^{(1)}\right| < \varepsilon \quad (2.21)$$

$$\left|\dot{x}_{k+1}^{(i+1)} - x_{k+1}^{(1)}\right| < \frac{\varepsilon}{T} \quad (2.22)$$

Where, ε is the vector of numbers repetitions.

The parameter γ checks the damping in the numerical integration:

- $\gamma > \frac{1}{2}$ - positive damping
- $\gamma = \frac{1}{2}$ - no damping
- $\gamma < \frac{1}{2}$ - negative damping

The beta (β) parameter should be a number within the range (0, 0.5). With $\gamma = \frac{1}{2}$, the following beta values for several integration methods can be achieved:

- $\beta = 0$ Second central difference.
- $\beta = \frac{1}{12}$ Fox-Goodwin's method
- $\beta = \frac{1}{6}$ Linear acceleration

- $\beta = \frac{1}{4}$ Constant average acceleration (trapeze method), unconditionally stable

2.3.2.1 Simple outline for solving equations of motion of a rigid floating body

The sea keeping problem for a rigid floating body in waves can be solved in the following steps, by finding:

1. The forces on the body with an arbitrary amplitude in calm water
2. The forces on the body when it is fixed on the incident waves
3. The mooring forces on the bod, if any
4. The dynamic equilibrium for each time instant when the sum of all the forces above is balanced in by inertia force of the accelerating body.

The forces acting on the body can be split into three different sources.

1. Fe – wave excited force on the fixed structure.
2. Fr – hydrodynamic reaction forces from the water on the body in motion
3. Frs – reaction forces from the connected lines (anchor, mooring lines etc.)

The hydrodynamic reaction forces i.e. the hydrodynamic properties of the body can be characterised as a mass-spring-damper system. Similarly, it also has three properties namely:

- A - Added mass due to deflection of surrounding water.
- B – hydrodynamic damping
- C – hydrostatic stiffness

The hydrodynamic reaction force can therefore be written as:

$$Fr = -A\underline{\ddot{\eta}} - B\underline{\dot{\eta}} - C\underline{\eta} \qquad (2.23)$$

The simple equation of motion now becomes:

$$(M + A)\ddot{\underline{\eta}} + B\dot{\underline{\eta}} + C\underline{\eta} = Fe + Frs \quad (2.24)$$

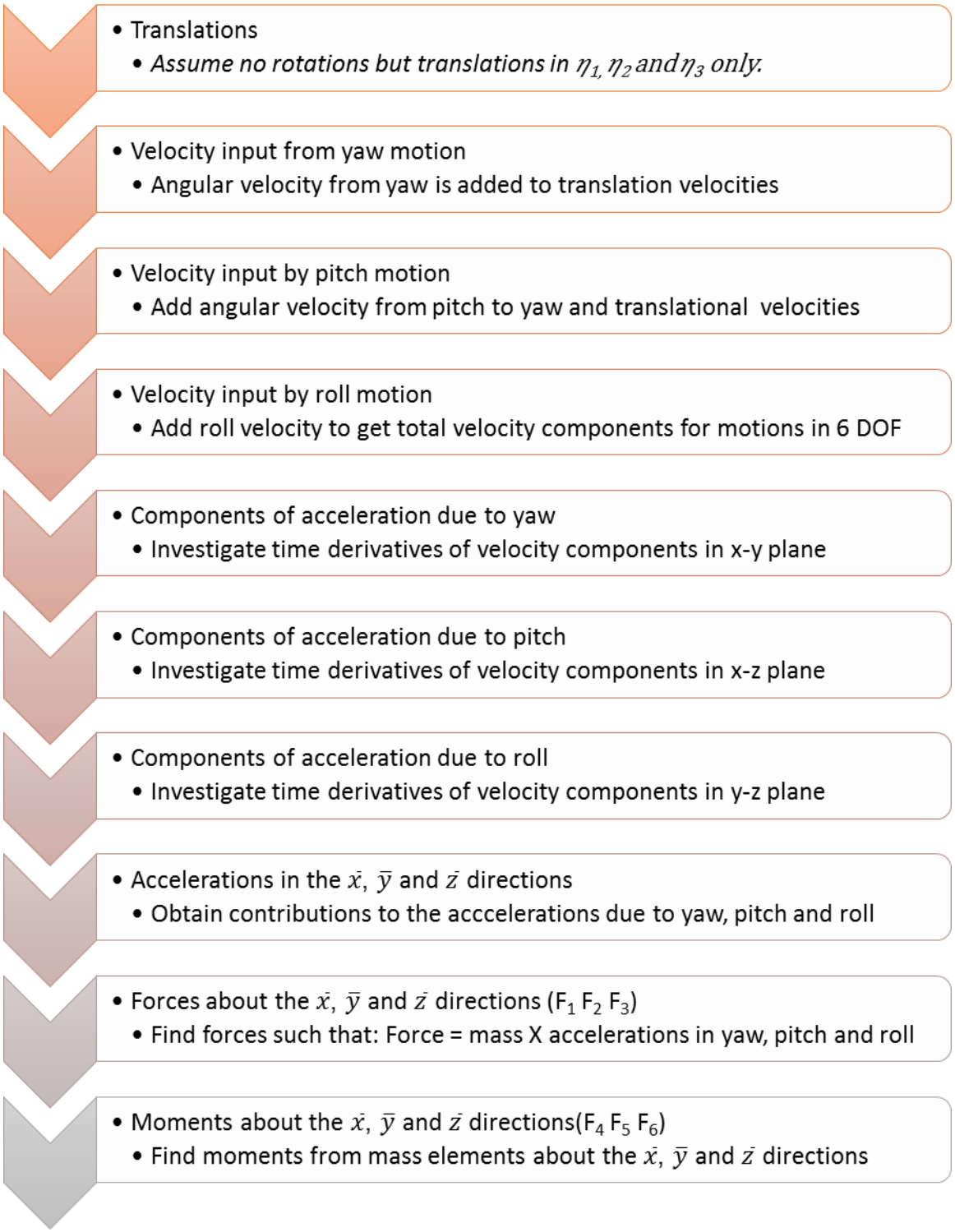

Figure 2.4 Layout of procedure for calculating vessel motions

Figure 2.4 Describes the steps in which the equations of motions are obtained for a floating body. The equations of motion for any arbitrary position of the coordinate system can now be obtained for all the forces and moments that correspond to the 6 degrees of freedom.

The sea keeping problem is then solved by the numerical methods using DeepC.

2.3.3 Model formulation in DeepC

The vector which contains the parameters for the location of the body is expressed as:

$$v = \begin{bmatrix} x \\ y \\ z \\ \psi \\ \theta \\ \varphi \end{bmatrix} \qquad (2.25)$$

The first three are coordinates of the origin of the floating (0, 0, 0) body in the earth fixed coordinate system.

From these coordinate, the model for body in motion is expressed in the form:

$$v = f(\ddot{v}, \dot{v}, \xi) \qquad (2.26)$$

Where ξ is a vector of parameters which are not dependent on the motion or non-motion of the floating body, e.g. propagation of waves and motion of current. In cases where the floating body is connected to another body or more, ξ vector will have the values of their velocities and heading1.

Consider the vectors:

$$\dot{v} = \begin{bmatrix} \dot{x} \\ \dot{y} \\ \dot{z} \\ \dot{\psi} \\ \dot{\theta} \\ \dot{\varphi} \end{bmatrix} \qquad (2.27)$$

$$\text{and } \ddot{v} = \begin{bmatrix} \ddot{x} \\ \ddot{y} \\ \ddot{z} \\ \ddot{\psi} \\ \ddot{\theta} \\ \ddot{\varphi} \end{bmatrix} \qquad (2.28)$$

The sub vectors $\begin{bmatrix} \dot{x} \\ \dot{y} \\ \dot{z} \end{bmatrix}$ and $\begin{bmatrix} \ddot{x} \\ \ddot{y} \\ \ddot{z} \end{bmatrix}$ represents the velocities and accelerations in the earth fixed system.

Let the angular displacements be expressed as $\omega = \begin{bmatrix} p \\ q \\ r \end{bmatrix}$ in the body system.

Therefore:

$$\dot{\psi} = p + q\sin\psi\tan\theta + r\cos\psi tan\theta$$

$$\dot{\theta} = q\cos\psi - rsin\psi$$

$$\dot{\varphi} = q\sin\psi\sec\theta + r\cos\psi sec\theta$$

$$\gamma = \begin{bmatrix}\psi\\ \theta\\ \varphi\end{bmatrix} \qquad (2.29)$$

$$\dot{\gamma} = f(\gamma, \omega) = M(\gamma)\omega \qquad (2.30)$$

Where $M = \begin{bmatrix}1 & \sin\psi\, tan\theta & \cos\psi\, tan\,\theta\\ 0 & cos\psi & -sin\psi\\ 0 & \sin\psi\, sec\theta & \cos\psi sec\theta\end{bmatrix}$ (2.31)

Taking derivatives with respect to time gives:

$$\frac{\partial f}{\partial \gamma} = \begin{bmatrix}(q\cos\psi - rsin\psi\,)tan\theta & (qsin\psi + rcos\psi)sec^2\theta & 0\\ -qsin\psi - rcos\psi & 0 & 0\\ (qcos\psi - rsin\psi)sec\theta & (qsin\psi + rcos\psi)\tan\theta\, sec\theta & 0\end{bmatrix} \qquad (2.32)$$

When, v , $\dot{v}$, and ξ are known, then $v = f(\ddot{v}, \dot{v}, \xi)$ is formed as follows:

1. The velocity vector $\begin{bmatrix}\dot{x}\\ \dot{y}\\ \dot{z}\end{bmatrix}$ is transformed to body-coordinate using the transpose of a matrix Δ
2. The ω is calculated from $\dot{\gamma}$ by M^{-1}.
3. The force $\boldsymbol{F_1}$ and moment $\boldsymbol{M_1}$ are computed from $\boldsymbol{x}$, $\boldsymbol{v}$, ω and ξ.
4. The acceleration results denoted by $\dot{v}$ and $\dot{\omega}$ are obtained
5. $\dot{v}$ is is transformed to the global system using the matrix Δ.
6. $\ddot{\gamma}$ is calculated.

Finally $\ddot{x} = (\dot{v}^T, \ddot{\gamma}^T)^T$ is formed. (2.33)

2.3.4 Coordinate transformation

The new orientation of the body is found by transforming its new coordinates after motion. It must be noted that the coordinates of the body is transformed from the earth fixed (global) to

the body fixed coordinate system before the motions are calculated. Hence the need to transform back to the original earth fixed coordinates system.

The orientation of the body coordinate system is regarded as being derived from an original to the global system or earth fixed by rotating it three times.

- The first rotation is by an angle ψ about the vertical z-axis. This changes the direction of the body's x and y-axes and corresponds to yaw motion.
- After that, the second rotation is by an angle θ about the y-axis. This changes the direction of the x and z-axes and corresponds to pitch motion.
- At the final step, the body is rotated by an angle φ about the x-axis, this changes the direction of the y and z-axes and corresponds to roll motion.

As a result, the position of the floating body in the body coordinate system is distinctively dependent by the angles by which it is rotated i.e. ψ, θ, φ with regard to the sequence by which it is rotated.

A vector's coordinates in the body coordinate system after calculating the motions can be determined by using a transformation matrix. This matrix transforms the coordinates of the new position to the representation in the earth fixed (global) coordinate system.

The transformation system is given as:

$$\Delta = \begin{bmatrix} cos\psi\ cos\theta & -\sin\psi\cos\varphi + \cos\psi\sin\theta\ sin\ \varphi & \sin\psi\sin\varphi + \cos\psi\sin\theta\ cos\varphi \\ \sin\psi\ cos\theta & \cos\psi\cos\varphi + \sin\psi\sin\theta\ sin\ \varphi & -\cos\psi sin\varphi + \sin\psi\sin\theta\ cos\varphi \\ -sin\theta & \cos\theta\ sin\varphi & \cos\theta\ cos\ \varphi \end{bmatrix}$$

(2.34)

Therefore a vector represented by $\bar{V}$ in the body coordinate system, the representation in the global system is:

$$V(G) = \Delta \times \bar{V} \qquad (2.35)$$

All position vectors are transformed by this procedure in order to read the results in the global system.

3 Dynamic positioning

3.1 Principles of DP

A dynamic positioning (DP) system has the responsibility to keep a floating vessel on a specified position, or to follow a moving object at a distance and a relative heading angle, or to move along a specified path. It incorporates measurements of the position and the heading and the controller with its control algorithms in order to utilize the propulsion system of the vessel accordingly. Furthermore the DP system aims to minimize the fuel consumption and the propulsion system deterioration during operation. (Balchen et al., 1980)

It should be noted that only motions in the horizontal plane of the vessel are "positioned", those being the surge, sway and yaw. Since only the vessel manoeuvring is of significance, the seakeeping problem is left behind during the process.

3.2 Common controllers

A number of control systems have been developed over the past few decades in order to increase the dynamic positioning performance. A very common group of controllers are the Proportional-Integral-Derivative (PID) type controllers, presented for the first time in 1922 by Nocholas Minorsky. It is based on a three-term control law with implemented low pass and/or notch filters to cut off the motion components from the wave frequency. Another widespread controller type is based on the Kalman filter theory for wave filtering. (Fossen, 2002)

3.2.1 PID controller

The PID controller is based on a three-term control law. For the control force from the thrusters F_{T0}, this law can be found in Marintek (2012a):

$$F_{T0}(t) = K_P * \varepsilon(t) + K_D * \dot{\varepsilon}(t) + K_I \int_0^t \varepsilon(\tau) d\tau \qquad (2.1)$$

The proportional control term is in charge of correcting the position error and its magnitude is proportional to the difference between the desired, x_0, and the filtered position of the vessel, x:

$$\varepsilon(t) = x_0 - x(t) \qquad \text{(Marintek, 2012a)}$$

Since the position feedback gain K_P is a constant, it can be seen that this term strongly influences the speed of transient response. Therefore a large positioning error results in a large thruster output and a zero error causes a zero output. Thus, this term is not enough for the system to reach a zero steady-state error. The addition of the integral feedback gain K_I can get the error to a zero steady-state. The contribution of the derivative control term depends on the rate of change of the position error; in case of dynamic positioning of marine vessels that is the change of velocity:

$$\dot{\varepsilon}(t) = \dot{x_0}(t) - \dot{x}(t) \quad \text{(Marintek, 2012a)}$$

With this in mind the velocity feedback gain K_D introduces phase lead to the system, as it accounts for the prediction of the position changing in time (Hellerstein, 2004).

In addition to that, the first-order wave disturbances are filtered out using a low pass and/or notch filter, because they induce oscillations, which go beyond the capacity of the thrusters.

3.2.2 Kalman filter-based controller

By contrast with the filtering used for the PID controllers, the Kalman filter implements linear optimal estimation theory for wave filtering that uses mathematical models to separate the vessel motions into low frequency (LF) and high frequency (HF) motions. Furthermore, the environmental forces from wind, waves and current are modeled, as well. This is done, because the heading and position measurements are distorted by signal and environmental noises. The HF motions due to first-order wave disturbances cannot be compensated by the thrusters and they only cause unnecessary tear and wear of the propulsion components and excessive fuel consumption. After filtering them out, only the slowly-varying disturbances are being positioned (Fossen, 2002).

The estimator determines a bias state of the system and the environment, which is updated at every step using the Kalman filter gains. The filtering and the state estimation are then used together with the controller feedback gain matrices to control the system. The system implements linearized kinematic equations of motion with predefined constant values for the yaw. (Fossen, 2002)

3.3 Effects of environment on DP

As a constantly changing entirety of multiple variables the environment has a significant role in changes of position and heading of a vessel. Wind and current directly affect the DP performance by applying large forces and turning moments with low frequency due to drag. The thruster allocation is constantly counteracting these in order to maintain a steady position and heading.

The wave environment is significantly different from wind and current with regard to its effects. It is known that the first-order wave forces are oscillating rapidly. Their contribution to the vessel motions is of high frequency, which cannot be countered by the thrusters and have to be neglected. Moreover, there are second-order wave forces attacking the hull. The mean and slowly varying of those act in the low frequency domain and can therefore be counteracted.

3.4 Control parameters

When it comes to the control system, the feedback gains have a huge influence in the outcome. They are basically factors that amplify the weight of positioning errors during the calculation of thruster output forces. It should be noted, that there is a set of control gains for each motion: surge, sway and yaw.

For the PID controller, the gains are easily recognizable in Eq. (2.1): K_P, K_I and K_D are the proportional, the derivative and the integral feedback gains, respectively. A mechanical analogy can be made, in order to adapt the control law to the dynamic positioning of a marine vessel. In this manner, K_P can be viewed as the wanted stiffness, and K_D – as damping coefficient of the motion. This interpretation could serve for the initial tuning of the controller. The values must be changed if the DP system doesn't exhibit the desired behavior. The integral feedback gain K_I comes in play for lower frequencies – if such are expected an upper limit ω_I should be set and K_I determined accordingly. Further considerations should be made for the low-pass and wave filters. (Marintek, 2012a)

Kalman filter-based controllers use a similar approach. There are two feedback gains per motion, these being the proportional and the derivative gains. A feedback gain from the current estimates provides the integral action of the controller and, in addition, there is a feed forward gain for wind compensation. These controller parameters determine the natural periods of surge, sway and yaw. (Balchen et al., 1980)

Significant difference between the two alternatives comes from the state estimator for the Kalman filtering technique. The estimator works with Kalman filter coefficients and innovations. These coefficients depend on the desired damping factors and cut-off frequencies for surge, sway and yaw. The innovations are the difference between estimated measurements and the actual position of the vessel. The mathematical equation for the Kalman filter coefficient matrix R (Marintek, 2012a) is:

$$R = \begin{bmatrix} 2\xi_x\omega_{c,x} & \omega_{c,x}^2 \\ 2\xi_y\omega_{c,y} & \omega_{c,y}^2 \\ 2\xi_\psi\omega_{c,\psi} & \omega_{c,\psi}^2 \end{bmatrix},$$

Where ξ is the damping factor; ω_c is the cut-off angular frequency, and x, y, ψ refer to surge, sway and yaw, respectively.

3.5 Gain settings for a Kalman filter-based controller

The relationship between the Kalman filter-based controller parameters and the natural periods of the compensated motions can be mathematically expressed as:

$$G(1,1) = -\left(\frac{2\pi}{T_x}\right) m_x \qquad G(1,2) = -2\xi_x\sqrt{G(1,1)m_x}$$
$$G(2,1) = -\left(\frac{2\pi}{T_y}\right) m_y \qquad G(2,2) = -2\xi_y\sqrt{G(1,1)m_y}$$
$$G(3,1) = -\left(\frac{2\pi}{T_\psi}\right) m_\psi \qquad G(3,2) = -2\xi_\psi\sqrt{G(1,1)m_\psi}$$

(Marintek, 2012a),

Where T is the desired natural period; m is the physical and added mass; ξ is the damping factor, and x, y, ψ are references to the surge, sway and yaw motions. A typical damping value is 70% of the critical damping and is therefore used in the later simulations (Marintek, 2012a). This leaves the natural periods as the only variable in the equation, thus giving control over the value of the feedback gain parameters. For surge, sway and yaw typical values vary between 60s and 90s (Marintek, 2012a). It is logical that faster motion

compensation demands a higher gain and it would result in a shorter natural period, and vice versa.

A slight remark should be made on the definition of gain. The theoretical insight is already explained. However, in practically oriented literature about dynamic positioned vessel gain is used as a rather abstract term. Usually it is only differentiated between low and high, and sometimes medium gain. These refer to the time-dependant positioning accuracy with the respective needed power output. For this reason, one can assume the practical meaning of the word as a summarisation of all the theoretically defined controller parameters with their relative capabilities to operate the DP system.

Throughout the rest of the thesis, gain is used in the practical sense of the word. A set of control parameters is chosen, which is attributed to wanted natural periods of 65s for the three controlled motions.

4 DNV SIMO

SIMO is software developed for frequency and/or time domain simulations of motions and station-keeping behaviour during offshore operations. Developed by Marintek, it is very flexible in its modelling capabilities. Vessels of different categories can be included in a simulation with a number of positioning systems and connecting mechanisms for. The programme provides comprehensive options for the environment with detailed definition of wind, waves, current and soil of the sea bed. For these and other reasons SIMO proves to be suitable software to study the given case, as well as it is preferred by many companies in the maritime industry.

The whole SIMO package is divided in different modules. The most significant ones are INPMOD, STAMOD, DYNMOD and OUTMOD. Each of them serves a different purpose essential to the whole process. They work in a logical order and every module creates output files, some of which are used as input for the next modules.

By default these file are named systematically in order for the modules to recognize them. The names consist of three parts: file type, system identifier and initial condition identifier (Marintek, 2012b). Essential input and output files for the respective modules are shown in Figure 4.1.

INPMOD, or the input module, needs external input, which contains the body data of the vessel, and input for environment, positioning systems, couplings, etc. The module reads body data from the result files of hydrodynamic programmes like WADAM. After the manipulation of the body data and the definition of the environment and other elements, which are to be included in the simulation, a system description file (SYSFIL) is produced by INPMOD. (Marintek, 2012b)

This system description file is then read by STAMOD, or the module that runs the static analyses. Alterations and manipulations of initial positions, positioning systems and restoring forces can be made once more. The static condition at time zero is then computed by STAMOD with an initial condition file (INIFIL) as output. At this stage, no more changes can be made. (Marintek, 2012b)

The next module in line is DYNMOD, which runs the dynamic simulations. The module reads the initial condition file and uses it as input for the analysis. Furthermore specific options and parameters should be chosen. DYNMOD generates the wave environment with the aid of Fast Fourier Transform (FFT) or cosine series, or a combination of the two. Wind gust is generated by FFT or state-space model and current can be used for the calculation of static force or force due to relative velocity. Other than that wave and wind time series can be read from a file. Before the simulation is run, the parameters for storage and the number and size of time steps are chosen. On completion a pre-generated data file and a time series file are written. (Marintek, 2012b)

OUTMOD serves the post-processing of the simulation. It needs the initial condition file from STAMOD, the pre-generated data and the time series from DYNMOD. The module presents the results and can analyse their statistics. An alternative is to use the module S2XMOD to export time series in file formats for programmes other than SIMO.

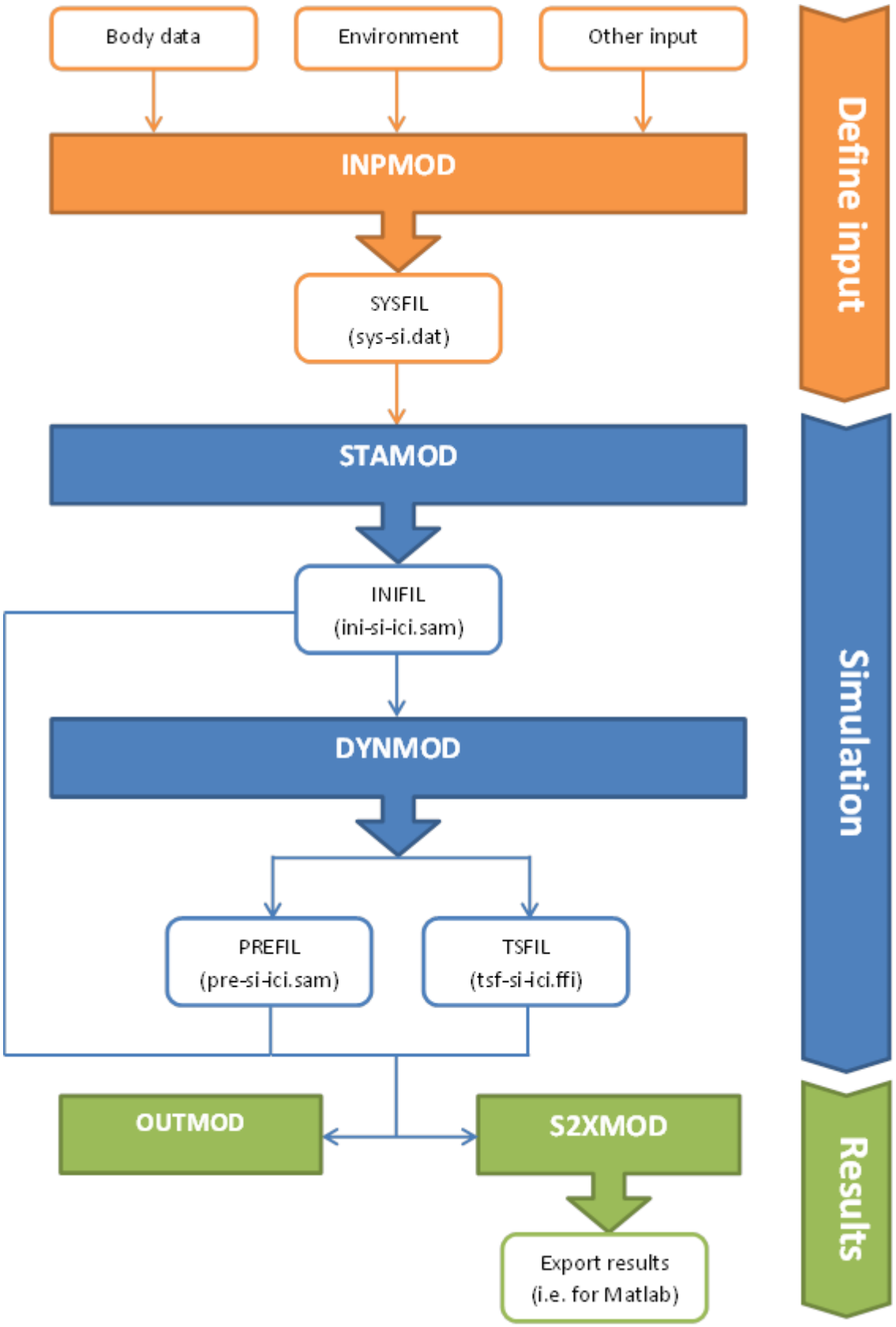

Figure 4.1 SIMO workflow and file communication and default naming; si = system identifier; ici = initial condition identifier

5 Vessel characteristics and set-up for simulation

The entire study is on the performance of the accommodation unit, floatel reliance when it is working alongside a Petrobras FPSO. This chapter seeks to introduce the two vessels in much detail.

5.1 Vessel characteristics

FPSO

PETROBRAS 35 was built in 1974 as JOSE BONIFACIO at Japan Marine United Corporation. It was later converted to a floating offshore installation with production unit in December 1988 at the Hyundai Heavy Industry Company limited in South Korea. The vessel is classed by the American Bureau of Shipping (ABS), see Table 5.1 (American Bureau of Shipping, 2015).

The FPSO operates in the deep waters of the Marlin field in the Campos basin off the coast of Brazil (PETROBRAS, 2015).

Table 5.1 Main Particulars of FPSO (American Bureau of Shipping, 2015)

Estimated Gross Tonnage	143742 tonnes
Length between Perpendicular (LBP)	319.9973 m
Moulded Breadth	54.4982 m
Moulded Depth	27.9989 m
Bulb Length from FP	7.71114 m
Length Overall (LOA)	329.312
Mooring System	Turret
Registered Owner	Petroleo Brasileiro SA
Class	ABS

The turret mooring system is composed of a fixed turret column supported by an internal vessel structure. The internal structure has a bearing arrangement to support free rotation. The components fixed on the vessel can therefore freely weather vane around the turret. The turret however fixed to its position by a number or anchor or mooring lines to the seabed (SBM Offshore, 2015).

This turret arrangement allows the FPSO to assume the direction of the least force against environmental loads (current, waves and wind). It consists of a swivel that allows for the transfer of fluids across the rotation interface while the FPSO is weathervaning. The concept of weathervaning is further explained in Section 6.3. On the working deck, located between the fixed turret column and the swivel, is a structure that supports the pipes and risers manifold. These manifolds mix up the fluids (oil, gas, water) and thus reduce the number of pipes and risers in the swivel stack.

FLOATEL RELIANCE

Floatel Reliance is a semisubmersible accommodation and construction support vessel designed built by Keppel Fels Limited in Singapore and delivered in the fourth quarter of 2010. It is capable of operating worldwide with a total accommodation capacity for 500 persons, see Table 5.2.

It utilizes dynamic positioning to maintain its position and heading when it is in operation. It is also classified by ABS with the class notation of A1, Accommodation Service, Column Stabilized Unit, Fire Fighting Vessel Class 2, AMS, and DPS-2.

Table 5.2 Main particulars for Floatel Reliance (Floatel International AB, 2014)

Length Overall	109
Breadth overall	68 m
Pontoon length	93.9 m
Breadth outside pontoons	45.2 m
Main deck height above base line	20.2 m
Draft excl 32thrusters(operation)	12.2 m
Draft incl thrusters	16.7
Displacement	18038 metric tonnes
Air gap	6.7 m
Main deck storage area	1300 m2
Dynamic Positioning	KONGSBERG K-Pos DPM-32
Thrusters	4 azimuth thrusters, each 2500kW
Mooring System	2 point wire mooring for inshore mooring.
Gangway	36.5 m with a telescopic action of +/- 6 m

5.2 Simulation models

The simulation model can be split into two sub models. They are:

1. A FPSO model for simulation of the FPSO vessel motion responses in a coupled analysis to obtain the time domain analysis in a given environmental condition.

2. A semi-submersible model for the Floatel Reliance also for the simulation of responses in a coupled analysis. In this model the gangway connection to the FPSO is considered as the line used in the coupling analysis.

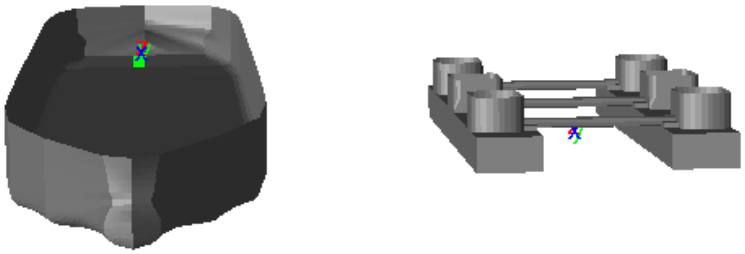

Figure 5.1 FPSO and floatel with lines models

Both models in Figure 5.1 are made up of the underwater part of the vessels. The FPSO is modelled in Autoship as a similar ship to the Petrobras 35 using information from the ABS records as given in Table 5.1 above. Due to the lack of relevant information to make a hydrodynamic analysis, the same wind and current coefficients found in the DeepC example file is used.

The Floatel Reliance model is provided by Floatel International AB along with other relevant hydrodynamic data and coefficients. The gangway is modelled as a 3-metre diameter line made of steel with its corresponding physical properties.

5.3 Setup

The system setup for the simulation in is shown in Figure 5.2. The floatel is situated on the portside of the FPSO with no lines attached. Instead it uses its DP system to keep a relative position to the FPSO and keep the gangway attached at all times as possible.

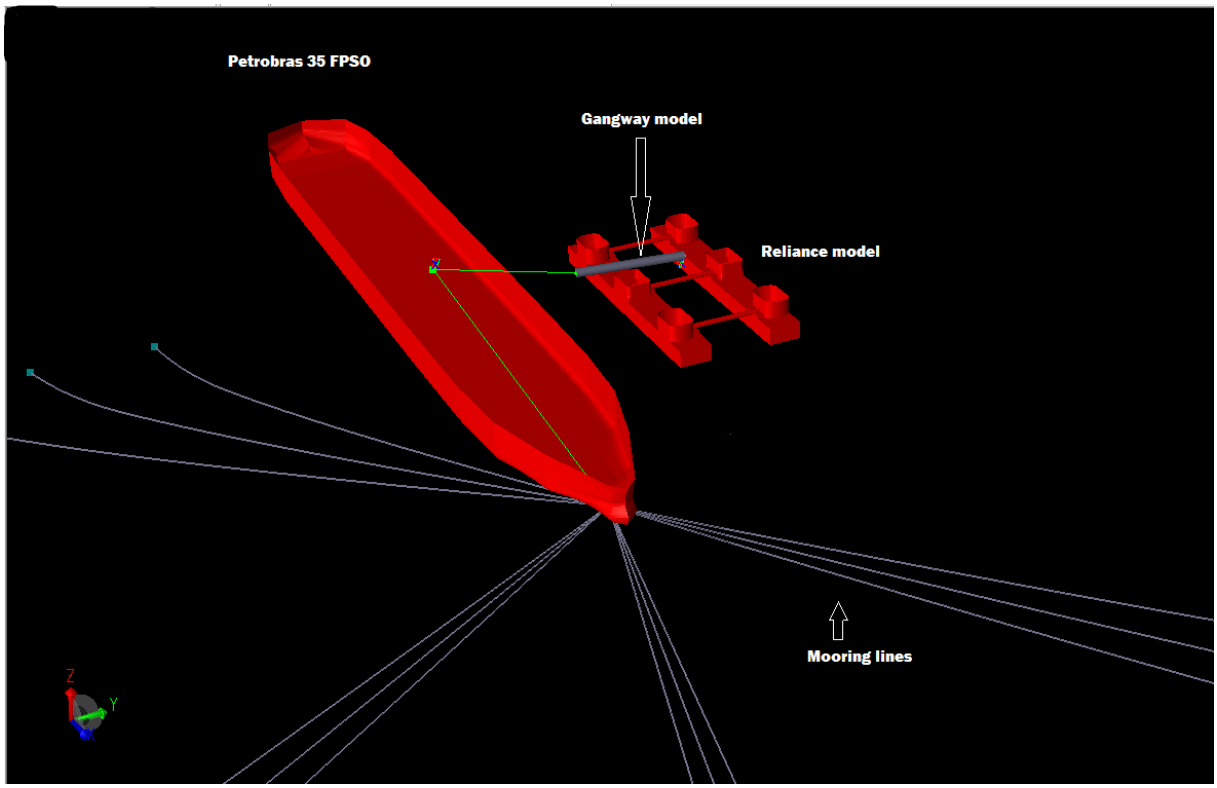

Figure 5.2 Layout of Simulation models

The thrusters' configurations are defined in the system description file. The loading condition for the FPSO is taken as the full load it can take while in operation with its corresponding draft. The floatel is also simulated in its operation displacement. The draft is however not including the height of the thrusters.

Since the same mooring system for the DeepC example file is used, the same water depth of 913.5 metres is also used. It surpasses the actual depth about 100 metres. Details of the environment are given in Chapter 6.

The environment information is taken from the vessel operation manual for a sister FPSO operating in the same location. Details about the environment are given in Chapter 4. A hydrodynamic model of the floatel is provided by Floatel International AB, the vessel owner.

The hydrodynamic model for the FPSO is obtained by modelling a similar vessel with the same characteristics as the Petrobras FPSO using Autoship. The information of the characteristics is found on the American Bureau of Shipping (ABS) public records. The vessel geometry is then created in DNV Sesam Genie and the hydrodynamic data is based on an example file from DeepC, however the mass data is from ABS records and the stiffness moments of inertia are calculated from that.

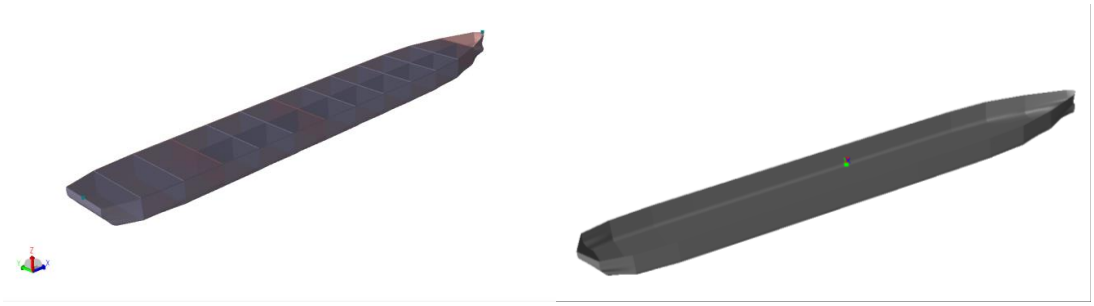

Figure 5.3 Similar FPSO models created in DNV Sesam Genie

The modelling of the various parameters is done with Det Norske Veritas (DNV) interactive software, DeepC. The DeepC software is an instinctive and novel program that employs the collaboration of two Marintek developed programs Simo and Riflex (Det Norske Veritas, 2013).

Simo program module calculates the floating body's station-keeping forces and the forces of the connecting mechanisms (mooring lines, gangway etc.). Riflex is responsible for the coupled analysis of the mooring system connected to the floating structure (DNV GL AS, 2015).

The simulations are done in two parts. The first part is the non-linear time domain coupled vessel motion analysis. In this simulation, the model of the FPSO alone with mooring lines attached in a turret mooring system is analysed in a particular environmental condition. This simulation is done in the DeepC GUI comprising of both Simo and Riflex. The result is a time trace and statistics of the vessel motions and line forces. For the purpose of this study, only the vessel motions or displacements and rotations are considered.

After the displacement results of the FPSO have been obtained, the floatel is simulated with prescribed motions obtained from the time series of the displacements and rotations of the FPSO. The second part of the simulation is done with the Simo software only. By this way, the complications of calculating connecting forces in DeepC are exempted to avoid errors since the floatel has no connection lines and that can be problem in Riflex. In this simulation, the DP system is added to simulation by entering the thruster configuration and the parameters for the controllers in to the system description file of the simulation.

6 Encountered weather environments description

6.1 Working location

The location of the vessel is off the south-eastern coast of Brazil called the Campos Basin. The Campos Basin is the main alluvial region which is part of the concession of petroleum giants Petrobras in Brazil. The region spans from the borders of Vitoria in the state of Espírito Santo stretching to Arraial do Cabo, which is at the upper strand of Rio de Janeiro. It covers a total area of around one hundred thousand square kilometres. (PETROBRAS , 2015)

All the meteorology and oceanography (Metocean) data used in this thesis is based on the Vessel operation manual for FPSO P-50. The environment modelling is made to include only the crucial factors that will determine the workability of the floatel. Environment modelling includes current profile, wave spectra, wind profiles, water depth of the location and the seafloor stiffness properties.

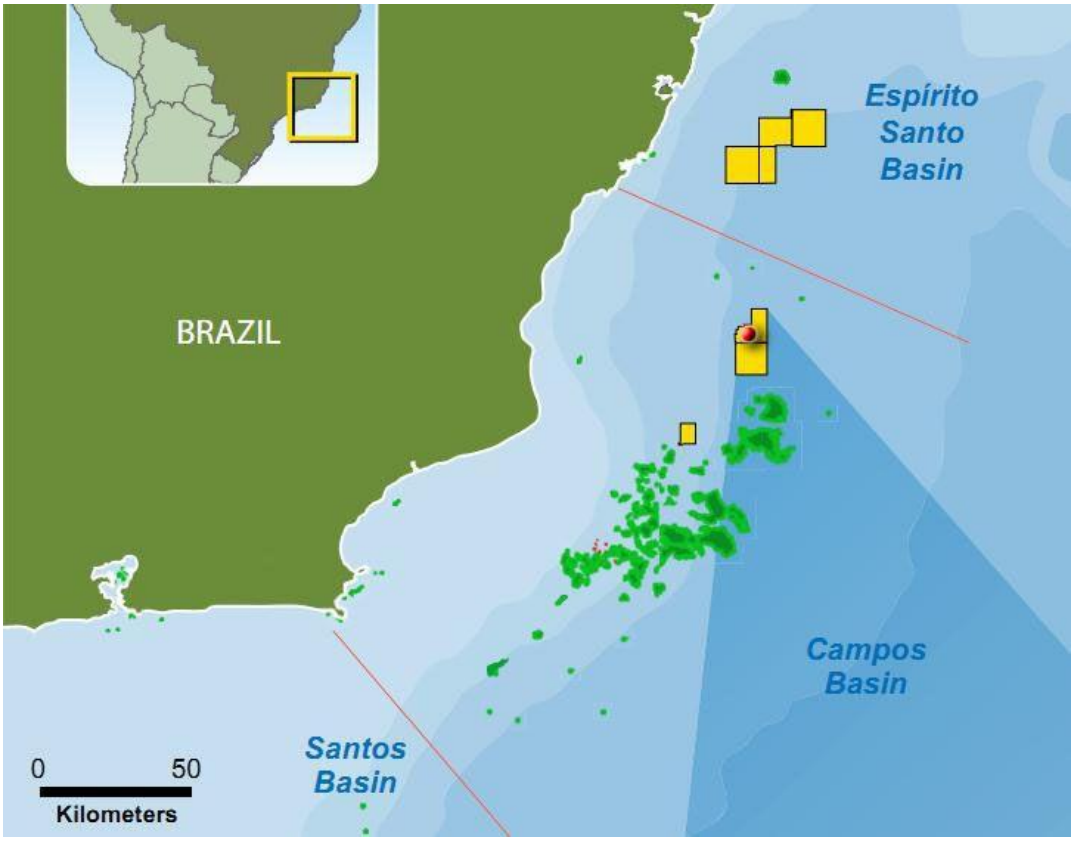

Figure 6.1 Campos Basin, Brazil (MercoPress, 2012)
The location, see

Table 6.1 has a water depth of 800 metres, however in this thesis a water depth of 913.5 metres is used for the analysis. The difference is not going to affect the outcome of the study since the performance of the DP system is the main focus and not the response of the FPSO in the coupled analysis.

Table 6.1 Environmental location containing site specific environmental data (Petrobras, Jurong Shipyard, & ForShip Engenharia Ltd, 2006)

Depth (mud line)	800 metres
Seabed property	Clay soil with 30kPa normal stiffness
Water density	1026 Kg/m^3 at 0-20metre depth
Seawater kinematic viscosity	1.19e-006 m^2/s
Air density	1.25 Kg/m^3
Air kinematic viscosity	1.462e-005 m^2/s

6.2 Environmental Conditions

In order to evaluate the performance of the DP system in the Brazilian sea water, a high quality study of the environmental conditions is particularly appropriate. The study of the environmental conditions will be limited to only the forces or loads that directly affect the performance. Other factors such as swell and tide which may add no impact on the performance of the system will be conveniently ignored.

For this reason the effects of current wind and wave are the three main forces that play a crucial role in evaluating the performance of the system.

The environmental condition for 4 key directions are based on suggesting's given by Floatel AB. The current is always considered to be coming from the same direction as a result of the weather vanning of the turret moored FPSO. The direction of the current is always simulated in the analysis with a heading of 0 degrees. In this thesis, the waves are considered to be directly generated and affected by local winds. The wind is also considered to be blowing during the entire simulation time. Therefore swells, which are wind-generated waves that continue to blow after the wind ceases are not included in the environment. The wind and waves are always simulated to be coming from the same direction. A non-collinear approach is adopted for the combination of the environmental conditions. The wind and waves are simulated in three main directions relative to the direction of the current. There are 90, 45 and 22.5 degrees. For each simulation, a combination of current coming from one direction and wind and waves coming from another direction as shown in Figure 6.2 is employed. These are done repeatedly for several cases of environmental conditions.

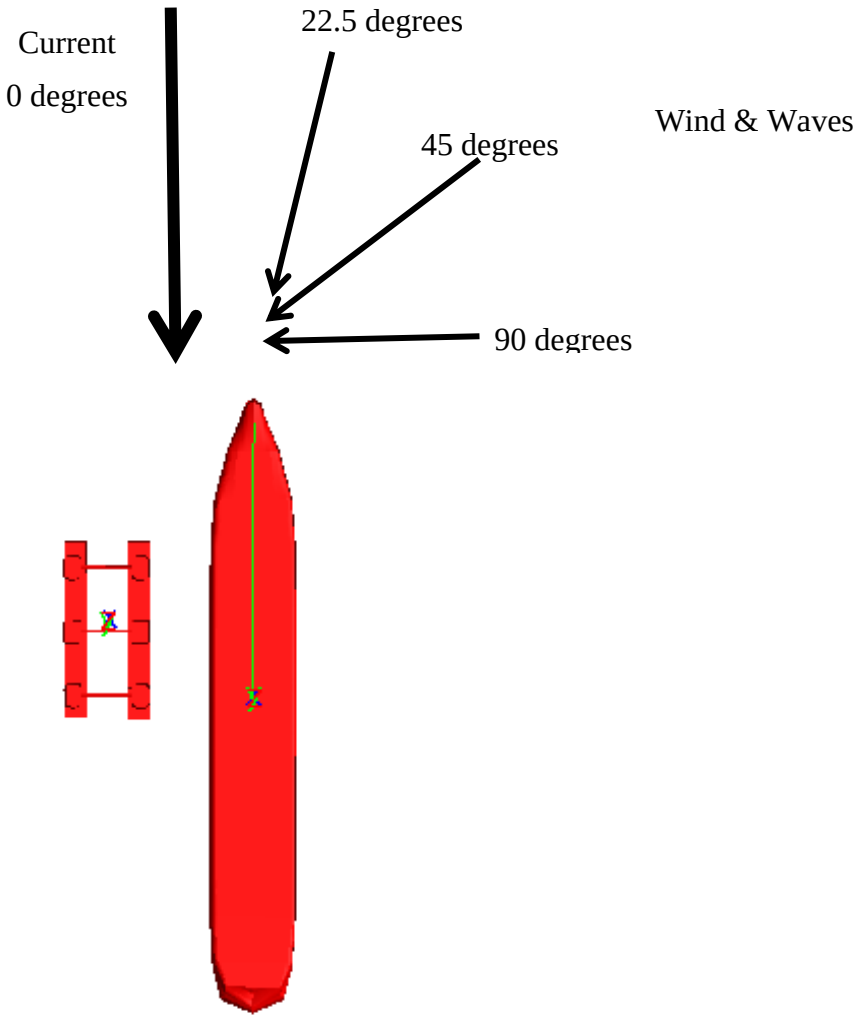

Figure 6.2 Environmental directions

Current

Aside from the directions, the current is simulated for 5 different velocities. The current profile gives a detailed description the velocities and corresponding direction of the sea measured at different heights from the bottom. The method of linear interpolation is employed. The current velocities as used in SIMO are assumed to be constant in the wave region, this is done by extending the current profile to the precise water level.They range from 0.75 to 1.5 m/s. The modelling of the current is done for the same direction i.e. 0 degrees throughout the vertical profile of the sea location. This is normally not the case as current reduces or changes in speed as the depth of the water increases and also due to the topography of the sea floor. The same assumption is done for the water density. As noted before, this will not affect the outcome of the thesis.

Waves

In the performance of offshore platforms, the most important properties are the vertical motions and accelerations caused by the waves in other words the disturbed free-surface-

level. They are vital in the estimation of equipment loads and also the possibility for personnel on board to live comfortably. Therefore in this thesis, the sea-keeping performance is decisive for the usefulness of the gangway connection. The downtime events for which the gangway is disconnected from the FPSO must be kept to the lowest minimum, if possible for only very extreme weather situations that are outside the workability of the dynamic positioning system (Janson, 2014).

Wave model

The linear wave potential theory or Airy wave theory is used for the simulations in this thesis. The generated incoming intact wave field towards the vessels is determined by the wave potential ϕ_0. The wave potential ϕ_0 represents a long-crested sinusoidal wave. This describes waves with very small wave amplitude compared to its wavelength and the water depth.

Unidirectional wave spectra are regarded as the total of a heavy number of regular waves transmitted at varying wave frequencies. Short-crested waves in the SIMO simulation are produced by adding a directional wave distribution to the wave frequency distribution (SIMO project team, 2012).

Airy's theory defines the wave potential as follows:

$$\phi_0 = \frac{\zeta_a g}{w} \frac{\cosh k(z+d)}{\cosh kd} \cos(wt - ktcos\beta - kysin\beta\phi_\zeta) \tag{6.1}$$

Where:

ζ_a	Wave amplitude
g	Acceleration due to gravity
k	Wave number
w	Angular frequency
β	Direction of propagation
ϕ_ζ	Wave component phase angle
d	Water depth

JONSWAP Spectrum

The Joint North Sea Wave Observation Project (JONSWAP) spectrum is an enhanced Pierson-Moskowitz spectrum. The Pierson-Moskowitz spectrum uses the concept of fully a fully developed sea where wind waves come to equilibrium when it blows over a large stretch of ocean for a long period. The JONSWAP spectrum uses an enhancement factor to account for the continuous development of the wave spectrum due to wave-wave interactions for a long stretch and period (wikiwaves, 2015).

The JONSWAP spectrum is expressed as:

$$S_{\zeta}^{+}(w)\frac{g^2}{w^5}exp\left(-\beta\left(\frac{w_p}{w}\right)^4\right)\gamma^{exp\left(-\frac{\left(\frac{w}{w_p}-1\right)^2}{2\sigma^2}\right)} \quad (6.2)$$

Where:

α	Spectral parameter
w_p	Peak frequency
γ	Peakedness factor
β	Form parameter
σ	Spectral parameter

Wind

The effect of wind is very significant in DP operation. The large area of the floatel and its high elevation makes it more prone to the effects of wind forces.

The wind field in the dynamic simulation is assumed to be 2-dimensional. That is it is transmitted as an area that is parallel to the water plane or water surface.

The wind model in DeepC includes the mean wind direction measured at a reference height.

The velocity of the wind has an unstable part in the mean direction and it is explained by the ISO 19901-1 also known as the Norwegian Petroleum Directorate (NPD) wind spectrum (SIMO project team, 2012).

The NPD spectrum is used for strong wind conditions at a reference height of 10 metres and an averaging time span of about 1 hour.

Wind profile

A wind profile showing the characteristics and statistics of the wind in the environment is implemented in the SIMO dynamic simulation. It can be described by the relation:

$$\bar{u}(z) = \overline{u_r}\left(\frac{z}{z_r}\right)^{\alpha} \quad (6.3)$$

Where

z	Level above the water
z_r	Reference to which the mean velocity is measured, normally at 10 meters
$\overline{u_r}$	Average speed at the reference height

α Height coefficient (0.10-0.14), For NPD wind spectra, Z_r is always 10 meters.

The wind profile is chosen from as the corresponding wind speed on a Beaufort scale for each of the significant wave height and time periods of the wave spectra that were chosen for the simulation Table 6.2.

Table 6.2 Wind speeds selected according to Beaufort scale (Met Office UK, 2015)

Significant wave height H_s [m]	Peak period T_p [s]	Wind speed u_w [m/s]
1.5	6	7
2.5	8	10
3.5	10	12
4.5	10	15

The average wind speed is calculated for each of the vessels as the wind speed at the reference height for which the wind force coefficients have been generated and included in the vessel data.

6.3 Weathervaning

The turret moored FPSO in this thesis, is a Single Point Mooring system (SPM) that allows the FPSO to weathervane freely about the mooring system, in response to the environment. This weathervaning ability allows the vessel to change its orientation with respect to the prevailing environmental direction to reduce the relative vessel-environment angles and the resulting load on the mooring (SOFEC, 2006).

The weathervaning ability offers numerous advantages in the operation of the FPSO. It reduces the motions at the bow end and makes it easier for offloading at the stern du the single point mooring.

The operation of the floatel is therefore expected to adjust to the swivel motion of the FPSO. The floatel must be able to follow the FPSO as it swivels in the transvers direction and at the same time counteract any environmental forces that act on it. In conclusion weathervanning provides an easy and inexpensive station-keeping procedure for the FPSO but comes as a challenge for the floatel that is required to follow the FPSO at all times in order to keep its gangway attached.

6.4 Focus and Assumptions

The focus is to asses study the most prevalent environmental conditions in the location. The analysis will not include extreme or rare weather conditions as the workability of the dynamic positioning system may even be out of range.

The following assumptions are also made for the simulations

- One direction for wind forces in entire simulation period
- No ocean swell in the location
- No wind gusts

6.5 Combination of Environmental conditions

The environmental data received from the operation manual showed generally an occurrence of mild conditions for most of the period recorded. The combination of current, wave and wind was done by combining mild current with high sea state and vice versa. The explanation of the cases is show in Table 6.3.

The table shows how the currents were combined with the wind and waves. In the preliminary simulations, it was noticed that the combination of strong currents and strong wind and waves (Case) were outside the operational limits of the thrusters (DP system). Therefore, in order to be able to simulate for strong wind and waves, the higher currents were combined with lower wind and waves and vice versa.

Table 6.3 Description of environmental cases

Case No.	**Significant wave height H_s [m]**	**Peak period T_p [s]**	**Wind speed u_w [m/s]**
Case 1	1.5	6	7
Case 2	2.5	8	10
Case 3	3.5	10	12
Case 4	4.5	10	15

Current velocity [m/s]	Direction wind/waves	Environmental case
0.75	22.5°	Case 2
		Case 3
		Case 4
	45°	Case 2
		Case 3
		Case 4
	135°	Case 2
		Case 3
		Case 4
1.00	22.5°	Case 2
		Case 3
		Case 4
	45°	Case 2
		Case 3
		Case 4
	135°	Case 2
		Case 3
		Case 4
1.25	22.5°	Case 1
		Case 2
		Case 3
	45°	Case 1
		Case 2
		Case 3
	135°	Case 1
		Case 2
		Case 3
1.50	22.5°	Case 1
		Case 2
		Case 3
	45°	Case 1
		Case 2
		Case 3
	135°	Case 1
		Case 2
		Case 3

7 SIMO Analysis of the Case Study

This section describes the approach for the simulation of the dynamic positioning of the floatel. It describes how the environment is created in SIMO, the manipulation of the system description file and the analysis of the results.

7.1 Modelling of the follow target case

The whole process of simulation was previously clarified in Chapter 1. This section expands on the explanation, so that every step of the analysis is clear. As reminder, the gangway has two connecting points – one on the FPSO and one on the floatel, and it can easily be represented by the distance between them. In the body fixed local coordinate systems they are $(x, y, z)_{FPSO}$ = (80, 25.25, 27.5) and $(x, y, z)_{floatel}$ = (44.94, -20.605, 27.5), respectively. In some cases the double symmetry of the floatel is taken advantage of by changing the body orientation around the centre of gravity by 180 degrees, in these cases the connecting point coordinates are corrected: $(x, y, z)_{floatel}$ = (-44.94, 20.605, 27.5).

After the motions of the connecting point on the FPSO are obtained from DeepC, these can be input in the simulation as a point with prescribed position. This is the point that is used as a reference point for the dynamic positioning system.

It should be noted that the FPSO is not located in the origin of the global coordinate system after the static analysis in DeepC. To properly execute the simulation, the floatel has to be relocated in a position, which allows for the distance between the two connecting points to be 36 m (gangway length with no shortening or elongation of the telescopic part). Additionally, the yaw angle of the floatel needs to be adjusted with respect to the relative angle between the vessels.

The new position and yaw angle of the semi-submersible are corrected in the system description file and STAMOD is initiated. The time domain simulation can now be launched using the produced initial condition file.

7.2 Generation of waves and wind

Floatel International AB has provided extensive information about the wave conditions in Campos Basin. These are presented in Chapter 4. In the simulation the waves were specified as irregular waves defined by the 3 parameters JONSWAP spectrum, using the significant have height H_s, the peak period T_p and the peakedness parameter γ. The latter is fitted to the local characteristics of the environment and can be calculated using

$$\gamma = e^{\left(1.0394 - 0.01966 * \frac{T_p}{\sqrt{H_S}}\right)}$$ (Petrobras, Jurong Shipyard, & ForShip Engenharia Ltda, 2006)

For the simulation of wind gust NPD spectrum is used, called also ISO 19901-1 spectrum. In order to define this SIMO needs the input for the propagation direction, average wind velocity and its respective reference height.

When SIMO generates the wind gust and the wave elevation, these are assumed to be Gaussian stochastic processes. During the analysis FFT was used for the time series of wind and waves. The Cooley-Tukey algorithm is implemented in the software to superpose the harmonic components with phases from a uniform distribution. The components are the result from the discretization of the variance density spectra of the wind and waves with equal frequency spacing and $N=2^r$ frequencies (r is an integer. (Marintek, 2012a)

The sampling of wind and waves is made at time interval 0.25 seconds. With simulation duration of 3 hours 43,200 samples for every parameter are computed, out of $N = 2^{16} = 65{,}536$ available.

7.3 Post-processing of the results

Given the nature of the study, the most important responses are the motions of the connecting points on both vessels, as well as the thrusters' power output for the dynamic positioning of the floatel. With the motions of the connecting point on the FPSO prescribed during the simulation only the time dependent global position of the floatel is of interest. DYNMOD computes that in the centre of gravity of the body, but OUTMOD easily transforms it in the coordinates of the connecting point.

There are two criteria, when it comes to the evaluation of every simulation: gangway length and the inclination of the gangway.

The undeformed gangway length is 36.5 meters. The capacity of the telescopic action is limited to +/-6 meters, but at 3 meters elongation or contraction an alarm indicates that the bridge should be detached. Therefore this criterion is set to 3 meters during the result evaluation.

In addition, the gangway inclination should also be monitored at all times. The inclination angle should not reach 3 degrees. It is measured relatively to the horizontal plane disregarding the local rotations at the connecting points on both vessels.

7.3.1 Gangway length

With the knowledge of the exact coordinates of both gangway ending points at every time step, the distance can be easily calculated:

$$dh = \sqrt{(x_1 - x_2)^2 + (y_1 - y_2)^2}$$

$$l_{Gangway} = \sqrt{dh^2 + (z_1 - z_2)^2}$$

$$Criterion\ (1): \quad l_{Gangway} \in (33.5\,;39.5)$$

Figure 7.1 shows the geometrical relationships of the connecting points' coordinates. In the figure, *P1* stands for the floatel connection, while *P2* – for the FPSO connection. The orthogonal projection of the gangway onto any given horizontal plane is named *dh*.

After the time dependent gangway length is calculated, it can be compared with the initial length of 36.5 m. Furthermore, if it's reduced by 36.5 meters, the result is the telescopic action of the gangway.

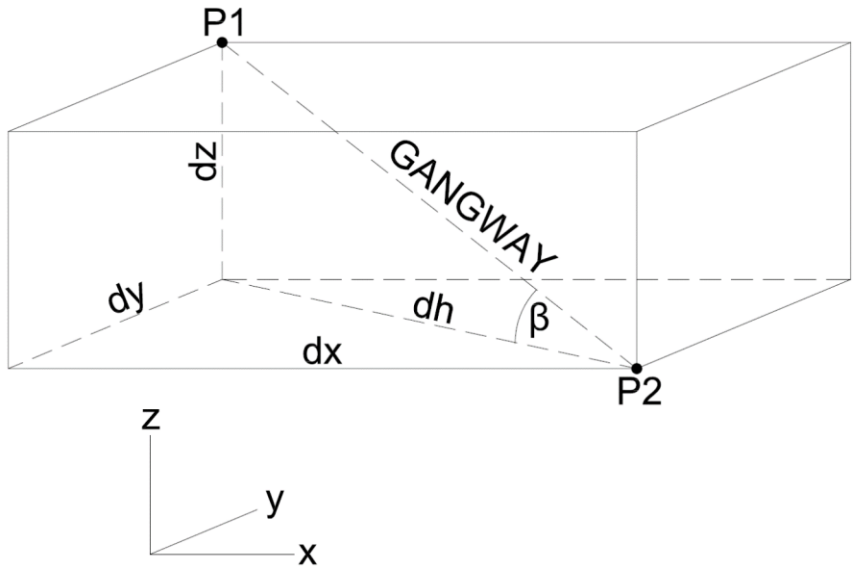

Figure 7.1 Simplified spatial model of the gangway

7.3.2 Gangway inclination

In Figure 7.1 the inclination angle is marked as β. The positive angle is defined for the situations, in which the connecting point on the floatel, P1, located higher than the one on the FPSO. No inclination, or β=0, occurs for the moments, during which both points are at the same height. This angle is easily found using the trigonometric ratios of the triangle locked by the sides "dz", "dh" and "Gangway". Their lengths are calculated during the examination of the first criterion. The angle can be found by:

$$\beta = \arcsin\left(\frac{dz}{l_{Gangway}}\right) = arccos\left(\frac{dh}{l_{Gangway}}\right)$$

$$Criterion\ (2): \quad \beta \in (-3\,;3\,)$$

The results from the different simulations are given in Chapter 8.

7.3.3 Validity of the simulated data

There are unreasonable fluctuations in the floatel motions during the first 15-20 minutes of the simulation. This can be clearly seen by plotting the gangway length for that time interval. An example is given in Figure 7.2.

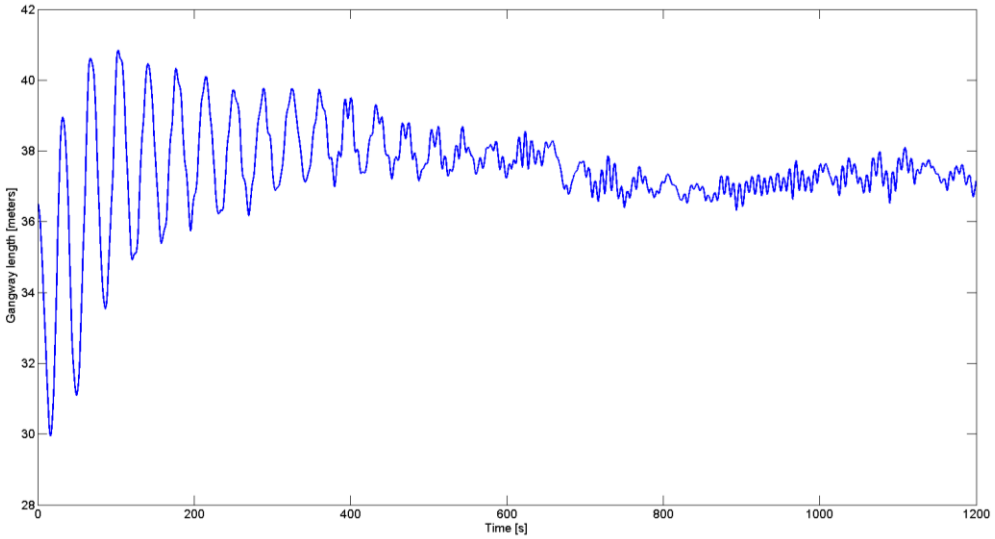

Figure 7.2 Large fluctuations of the gangway length due to the initial state of the Kalman filter estimator, before it adjusts to the environment

Despite the disturbing occurrence, the explanation is rather mundane. The Kalman filter estimator needs some time to catch up on the trends of motion, which allows the controller to coordinate the mathematical model with the environment and the moving point. Simply put, it is a "warm-up time".

For the purpose of presenting plausible results, the first 20 minutes of samples are disregarded from the simulated data. Therefore, all the graphs in this section begin from the 1200th seconds. Compared to the total simulation length (10800 seconds) and considering, that there are 4 samples per second, the trimmed data should suffice for valid conclusions.

8 Results

In Chapter 5 the analysis process with its distinct features was elaborately described. This chapter focuses on the outcome by presenting the results for various simulations.

The first part aims to exhibit how the three different orientations between the floatel and the FPSO influence the output thrust needed for the positioning. This is done in consideration of the following target objectives. The comparison of these allows making a statement about a preferable relative angle between the vessels, depending on the direction and severity of the environment.

In sequence parts of time series from some simulations are used to illustrate how the thrusters control the motions of the accommodation unit in order to assure that the DP footprint stays within limits set by the gangway stroke.

Finally, a study on the correlation between the gangway length and inclination and the floatel motions is done. The aim here is to demonstrate how the semi-submersible reacts to the FPSO with regard to each motion causing the vessels to float as a "collaborate" system, held together by the passage.

8.1 Total thruster forces

The four azimuth thruster installed wok in synchrony to achieve two goals. Firstly, they have to compensate the motions, cause by the environment and, secondly, they have to keep away from the FPSO at constant relative distance and angle.

That is a cost-intensive operation, therefore the thrust output is of great interest. A careful and detailed analysis could immensely reduce the running costs: A comprehensive knowledge about the DP system capabilities and proper utilization of the power capacity combined with the information on power demand for various situations at sea can be a decisive factor here. On the one hand the income from the operation is directly dependent on the time, during which the floatel is connected to the FPSO. On the other hand maintaining this connection could demand full power output, which would then maximise the expenses, thus reducing the profit.

An overview of the mean total thruster forces for all the simulations is given in Tables 8.2 and 8.3. In order to properly compare these for the different environments and orientations, the same DP controller settings are used for every simulation. Naturally, this results in inconsistent deviations from the position. But since the thrust forces are the focus, the gangway stroke and inclination are looked upon as secondary criteria. For that reason minor violations of the limits are ignored in cases with enough thrust capacity to counteract these, given a specific tuning of the DP controller. At the same time cases, in which the full capacity of the positioning system is not sufficient to perform the operation and the distance between the vessels is constantly growing, are omitted from the tables. With this in mind, note how the higher current velocities deplete the thrust capacity at lower sea states, hence the difference sea states for the 1.25 and 1.50 m/s currents. As for the environmental cases used, the current and wind/wave directions are given separately. The case numbering used in the thesis only contains the significant wave height, the peak period and the wind speed. These can be found in Table 8.1.

Table 8.1 The four different environmental cases used for the simulations. The directions are not included in the case definition

Case No.	Significant wave height H_s [m]	Peak period T_p [s]	Wind speed u_w [m/s]
Case 1	1.5	6	7
Case 2	2.5	8	10
Case 3	3.5	10	12
Case 4	4.5	10	15

Table 8.2 This table shows the mean of the total thrust force for all the simulations with current velocities 0.75 and 1.0 m/s

Environment			Mean total thrust force		
Current velocity [m/s]	Direction wind/waves	Environmental case	Parallel orientation [kN]	Diagonal orientation [kN]	Perpendicular orientation [kN]
0.75	22.5°	Case 2	285	490	572
		Case 3	332	571	667
		Case 4	460	735	886
	45°	Case 2	285	461	549
		Case 3	339	535	636
		Case 4	453	683	834
	135°	Case 2	208	340	440
		Case 3	329	402	483
		Case 4	399	470	602
1.00	22.5°	Case 2	376	731	823
		Case 3	414	795	905
		Case 4	313	959	1124
	45°	Case 2	390	705	808
		Case 3	435	761	881
		Case 4	560	901	1073
	135°	Case 2	313	576	682
		Case 3	375	594	690
		Case 4	493	662	822

Table 8.3 This table shows the mean of the total thrust force for all the simulations with current velocities 1.25 and 1.5 m/s

Environment			Mean total thrust force		
Current velocity [m/s]	Direction wind/waves	Environmental case	Parallel orientation [kN]	Diagonal orientation [kN]	Perpendicular orientation [kN]
1.25	22.5°	Case 1	376	931	971
		Case 2	681	1537	1669
		Case 3	510	1086	1208
	45°	Case 1	684	905	979
		Case 2	479	989	1097
		Case 3	538	1044	1183
	135°	Case 1	351	846	919
		Case 2	429	885	1006
		Case 3	466	893	1041
1.50	22.5°	Case 1	496	1285	1337
		Case 2	597	1384	1488
		Case 3	644	1508	1883
	45°	Case 1	482	1261	1336
		Case 2	590	1343	1453
		Case 3	654	1398	1544
	135°	Case 1	450	1191	1267
		Case 2	551	1248	1535
		Case 3	600	1266	1423

All the simulations are used to compare how the relative angle between the floatel and FPSO influences the thrust output force. By putting together various environmental cases and directions a trend can be found, which provides essential information for the choice of preferable orientation. Figure 8.1 demonstrates this trend in the example of current velocity of 1 m/s: For all the three directions of wind and waves it can be conformed that the parallel orientation demands the lowest level of thruster output, followed by the diagonal orientation by large margin. It is indisputable that a perpendicular orientation of the floatel to the FPSO leads to the highest thrust forces, about twice as much as the thrust needed for the parallel scenario.

Another trend that shows is the rather small increase of the power demand for the DP system with the growing height of the waves. When it comes to thrust force as criterion, the operation could seemingly be performed at much higher seas, as well. However, the secondary criteria here are the gangway length and inclination and should be kept in mind for any prediction on the working conditions limitations. The simulations are done for significant wave heights up to 4.5 meters not because of power insufficiency, but because the inclination of the gangway becomes a problem. At this wave height the limit of +/- 3 degrees is exceeded multiple times. The only reason the results from these simulations are used relies on the focus of the study: thruster output.

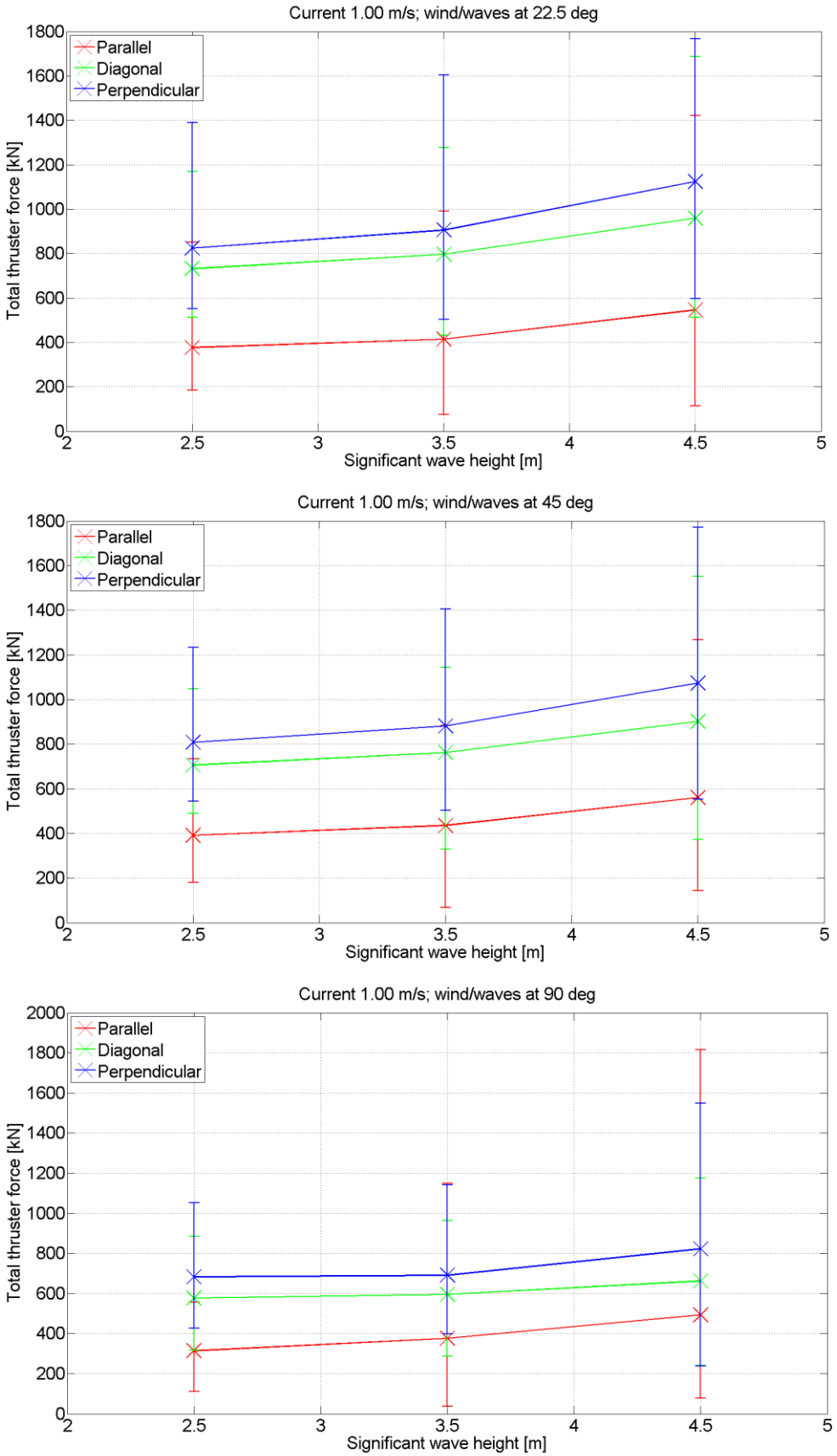

Figure 8.1 The figures show the comparison of the mean, maximum and minimum value of the thrust forces during the 3-hour simulations for each of the different orientations. They also demonstrate the increase of the thruster output force due to changes in the sea

It can now be established that the lowest thrust output forces is expected for the parallel orientation. A more comprehensive exhibition of the thrust for this most preferable relative angle is shown on Figure 8.2. This is the example for environmental case 3. It is evident that the direction of the wind and the waves has only small influence on the power output. Slightly higher impact is made by the growing current velocity.

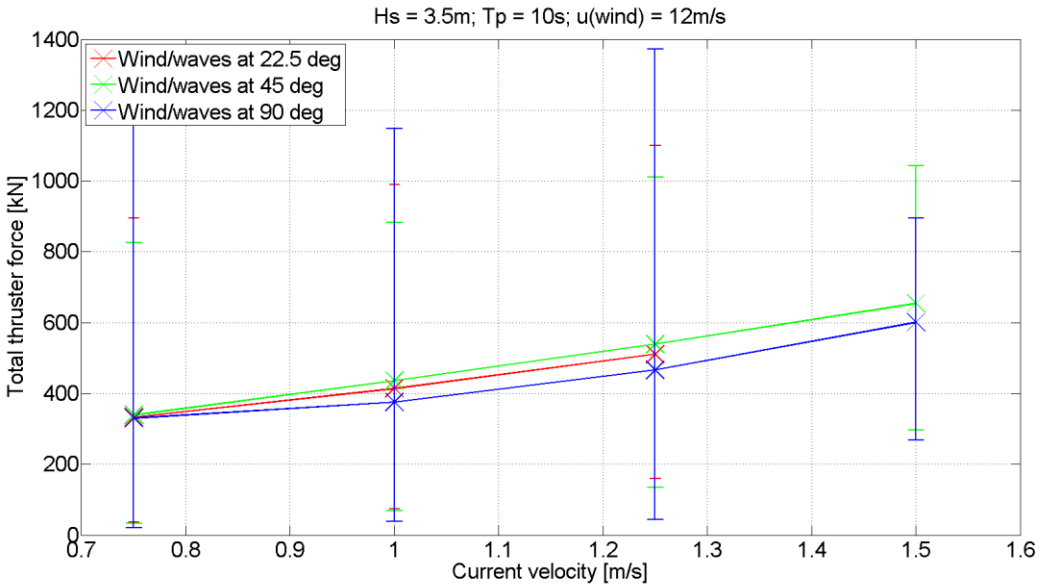

Figure 8.2 Increase of the thrust force for faster current velocities. The graph examines the parallel orientation of the vessels

8.2 Motions of the vessels

This section reviews the motions of the floatel alongside the FPSO with regard to the thrust forces and gangway length and inclination. Alongside is a key word here, as the DP system strives to mimic the motions of the FPSO. It is very important to note that the FPSO assumes an initial position after the static simulation. At the static position, the turret mooring system secures the FPSO from drifting away. The direction of the most dominant environmental load (in this case, the current) is shown by the set of mooring cables with experiencing the highest tension force or relative axial elongation as shown in figure 17 and figure 18. Since the weather vanning adjusts the vessel to the current head on, the forward set of mooring lines is the most effective in securing the FPSO in place therefore experiences the most tension. As a result, the FPSO does very little surge motions from forward current but undergoes mostly sway or swivel motions due to wind and waves coming at a different angle.

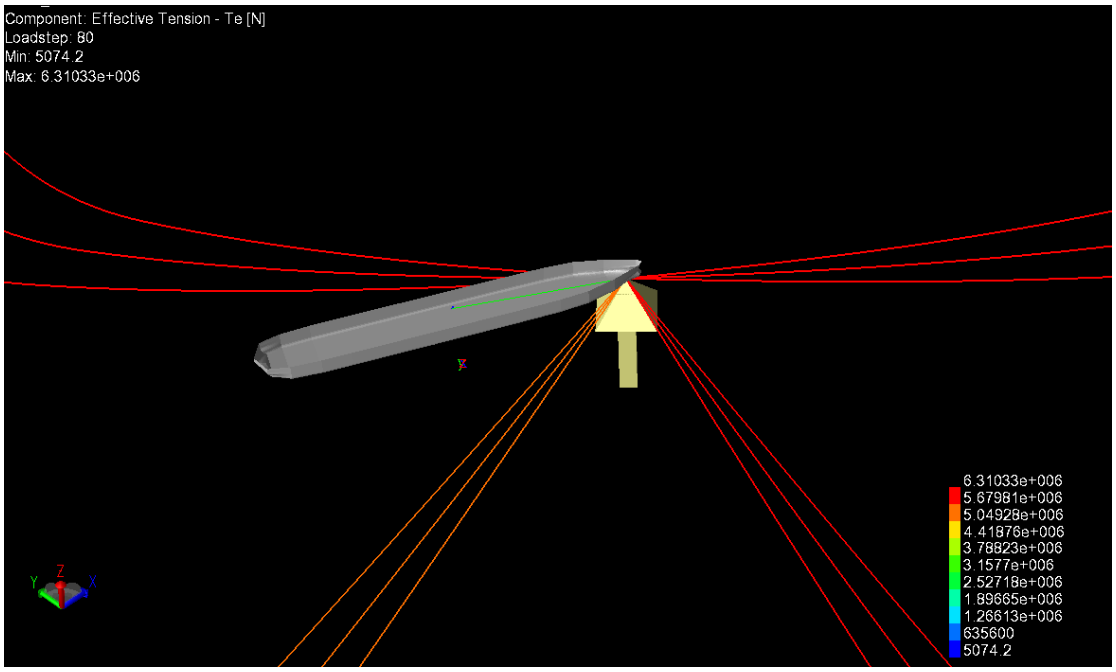

Figure 3 Effective tension on mooring lines of >FPSO due to weather forces

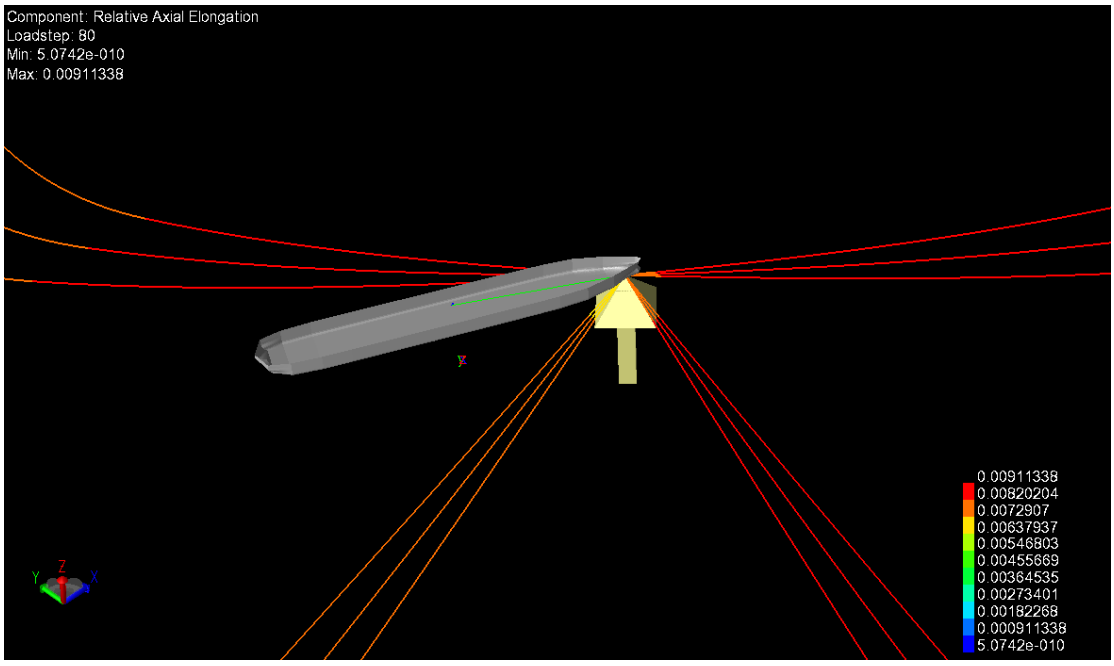

Figure 4 Axial elongation of mooring lines due to forces from weather

Unlike the FPSO, the Floatel uses thruster force to counteract all environmental loads as well as keeping its position relative to the FPSO. In this regard, the thruster works mostly in the direction of the forward current force for most of the time and the rest to follow the sway/swivel motions. As more thruster force is used to counteract forward loads, it is also important to position the floatel so as to have the least resistance in its forward motion. In perspective, all loads acting on the FPSO is represented on the floatel and the thrusters are used to neutralize them in order to sync their motions. In an ideal situation these would behave as two rigidly connected hulls. However, the differences in mass, hydrodynamic and aerodynamic properties, phase shift of the attacking waves, etc. prevent this from happening.

Despite that the motions of the accommodation unit are conformed to the FPSO at all times. This is clearly visible in Figure 8.3. The figure shows a short interval of the simulation for environmental case 2 with current velocity of 1.5 m/s and wind and waves coming at 22.5 degrees. Naturally there is a large offset between the two sway curves in direction of the vertical axis. That is due to the distance between the vessels. But there is also a small offset along the horizontal axis of the graph. This is the time lag in the response of the DP system. In this example, by comparing the dips of the two curves, the lag can be estimated to about 60 seconds. It is attributed to the thrust forces, despite being hard to notice. But sudden changes in the thrust curve are clearly responsible for changes in the sway of the floatel. This is observed in very short periods.

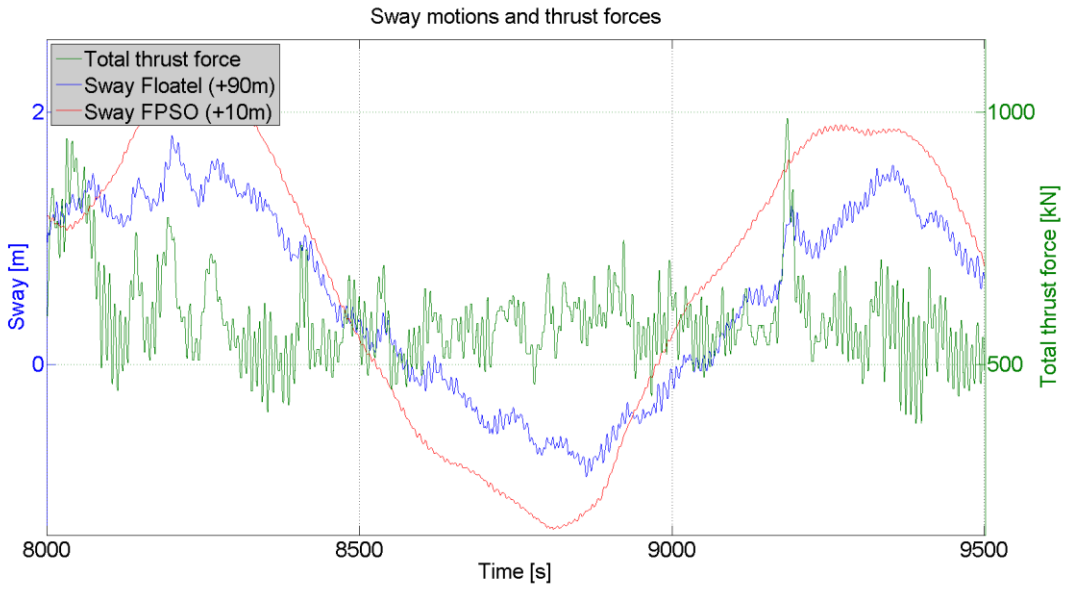

Figure 8.5 The conformity of the floatel sway to the FPSO and the respective total thruster output. Parallel orientation

Table 8.4 gives the correlation factors for all motions and the gangway stroke for the same example. The numbers in it agree with the whole scenario of the simulation. Firstly, the correlation between sway and yaw tangibly differ from that of the surge motions. To understand this, it should be reminded that the parallel orientation means just about head seas, therefore the surge motion is strongly influenced and it deviates the most for the two vessels. Secondly, the lower correlations of the FPSO motions to the gangway stroke imply that it is being followed and the accommodation unit has to correct the elongation.

Table 8.4 Correlation factors for parallel orientation. Current: 1.5 m/s; case 2; waves and wind at 22.5 degrees

	Gangway stroke	**Surge FPSO**	**Sway FPSO**	**Yaw FPSO**
Gangway stroke		-0.40	-0.41	0.41
Surge floatel	-0.50	0.68		
Sway floatel	-0.20		0.96	
Yaw floatel	0.51			0.92

If the wind and waves change the direction to 45 degrees the correlation factors change accordingly. This can be seen in Table 8.5. In this situation the dependence of the gangway stroke on the sway of the floatel is growing as the motion becomes more vast due to the stronger lateral loads from the environment. In general, the sway motions continue to be highly correlated keeping the distance between the vessels in check.

Table 8.5 Correlation factors for parallel orientation. Current: 1.5 m/s; case 2; waves and wind at 45 degrees

	Gangway stroke	Surge FPSO	Sway FPSO	Yaw FPSO
Gangway stroke		-0.41	-0.38	0.42
Surge floatel	-0.51	0.7		
Sway floatel	-0.28		0.89	
Yaw floatel	0.5			0.92

Changing the environmental direction once again, a new scenario envelops. Examining the surge motions co-dependency in Table 8.6 shows that they are much more in tune. The reason is the reduced loads acting in longitudinal direction on the floatel, thus allowing easier counteraction from the DP system. This high correlation is shown in Figure 8.4. The thruster force curve has seemingly low correlation to the sway here. This is attributed to the composition of the curve itself: It is the sum of the forces from four thrusters acting in various time-dependent directions.

Table 8.6 Correlation factors for parallel orientation. Current: 1.5 m/s; case 2; waves and wind at 90 degrees

	Gangway stroke	Surge FPSO	Sway FPSO	Yaw FPSO
Gangway stroke		-0.38	-0.37	0.37
Surge floatel	-0.283	0.977		
Sway floatel	-0.255		0.977	
Yaw floatel	0.373			0.990

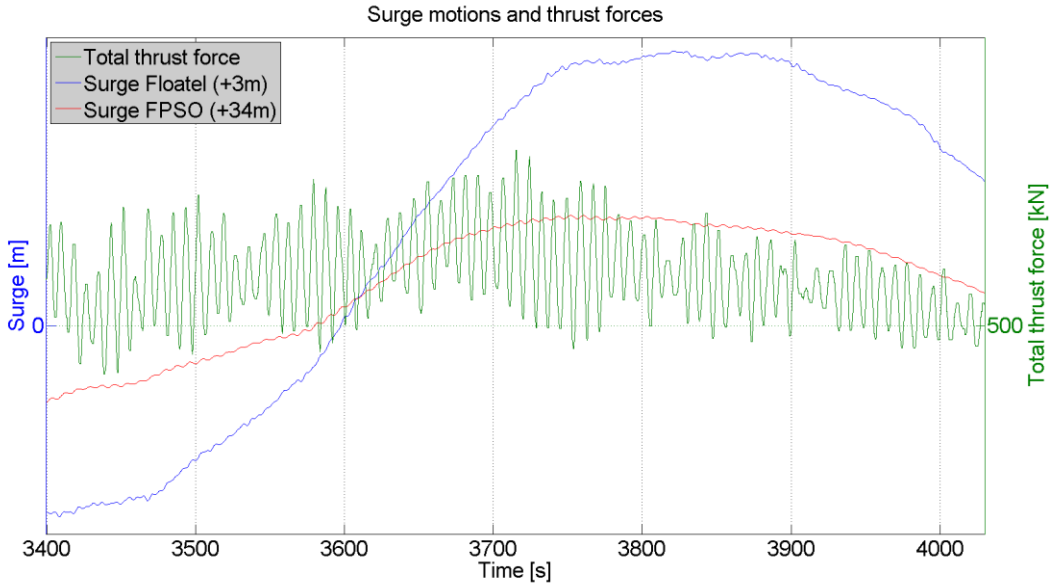

Figure 8.6 The surge motions of the vessels are highly synchronised in this example. The correlation can be read in the table above

It should be noted that the yaw angles of the vessels are consistently in synchrony. By rule, the heading is prioritised in the setting of the DP controller parameters. This becomes obvious by comparing the correlation factors of the yaw motions in the tables previously reviewed. Four thrusters located at the ends of the pontoons can provide yaw moment at fast rates and large magnitudes, thus making it easy to control. It is however hard to recognise from the total thrust force curve. An example for this trend is given in Figure 8.5.

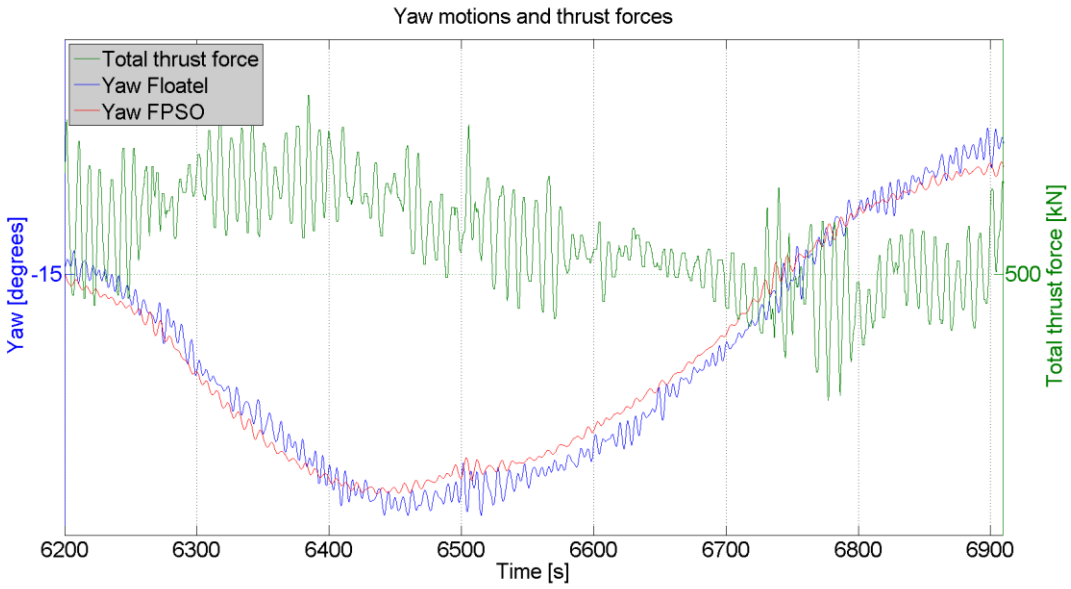

Figure 8.7 Yaw of the floatel in strong correlation to the FPSO rotation

9 Conclusion

The thesis project is set up to study the main concerns with respect to the DP operation of an accommodation floating platform (namely a floatel), i.e. the best orientation for the floatel pontoons that will require less power for the follow target operation whilst keeping the gangway connected to the FPSO.

The simulations in DeepC and SIMO have provided a variety of results for the different weather conditions. Even though some of the simulations were unsuccessful due to computational errors, there are enough to make some general conclusions to reflect the overall objective of the thesis project.

The results present a comparison of the thrust forces produced by the thrusters of the floatel in order to maintain a fixed distance to keep the gangway connected. For the three orientations of the pontoon that were suggested, the results show a trend of lower mean total thrust force for the parallel orientation. For example, in the simulation of a current speed of 1.5m/s with perpendicular direction of the average wind speed and significant wave height of 12m/s and 4.5m, respectively, the results show the following:

The percentage of the total thrust capacity used as the mean power during the simulation is

- 35% for the parallel orientation
- 74% for the diagonal orientation
- 83% for the perpendicular orientation.

It is seen that positioning the pontoons parallel to the turret moored FPSO requires less thruster force for DP operation relative to the weather vanning FPSO. As mentioned in the earlier chapter the weather vanning adapts the heading of the FPSO to the most predominant environmental force. With the floatel using a similar heading as the FPSO, the drag coefficient of the pontoon is significantly lowered. The reference area of the pontoon to the resistance for the environmental forces to act on is reduced to the longitudinal ends of the pontoon. The other orientations create a larger area with respect to resistance drag.

From this observation, the floatel operating in parallel orientation to the FPSO will allow for the thrusters to utilize less force in balancing environmental forces due to wind, waves and current acting towards the heading of the FPSO. These forces will be significantly reduced and rendered trivial by proper positioning of the pontoons.

This leaves more thrust force capacity to follow the motions of the FPSO.

10 Recommendations

The implications of the results presented in this thesis may be regarded as considerable for improving the operating condition of the floatel and reducing downtime events. From the given problem scenario i.e. environmental loads, set up of FPSO to be followed and all other situations considered in the analysis, this report suggests that the floatel should use the same heading as the FPSO. The parallel operation will allow the floatel to mimic the weather vanning operation of the FPSO therefore 'adapting' its heading to the prevailing environmental load. This will allow the floatel to achieve similar advantages in station keeping analogous to a weather vanning vessel.

The major factor for gangway disconnection is the limitation of thruster force in follow target operation. This orientation will allow less environmental loads on the pontoon and reduce operation cost from fuel consumption. There will be more thrust force available for follow target ability which is very important in preventing gangway disconnection.

11 Future work

One major factor to note is that the thesis was carried out using environmental data irrespective of time of year or season. It would be beneficial to make a study of the monthly operational conditions or workability of the floatel using the related environmental data. This could help decide the DP control parameters to be used according to the time or season. This form of operation if utilized by the operator can help cut down the running cost of the floatel.

The environmental loads i.e. wind and waves in this thesis were always assumed to approach from the side of the FPSO. It is crucial to consider similar analysis in this thesis but with the wind and waves acting from the side of the floatel. The current study showed fairly good performance of the floatel in slightly rough environment notwithstanding the possible effects of wave diffraction needs to be investigated.

For further optimization of the performance of the floatel, it would be essential for the pontoons to be streamlined to improve the hydrodynamic properties and reduce the frictional drag.

12 References

Balchen, J. G., Jenssen, N. A., Mathisen, E., & Sælid, S. (1980). *A dynamic positioning system based on Kalman filtering and optimal control*. Modelling, identification and control, 1980, Volume 1, No.3, 135-163

Fossen, Thor I. (2002). *Marine control systems: Guidance, Navigation, and Control of Ship, Rigs and Underwater Vehicles*. Marine Cybernetics. Trondheim, Norway

Marintek. (2012a). *SIMO – Theory Manual Version 4.0 rev. 1*. Norwegian Marine Technology Research Institute. Trondheim, Norway

Hellerstein, Joseph L., Diao, Yixin, Parekh, Sujay, Tilbury, Dawn M. (2004). *Feedback Control of Computing Systems*. John Wiley & Sons, Inc.

Balche, Jens G., Jenssen, Nils A., Sælid, Steinar. (1976). *Dynamic positioning using Kalman Filtering and Optimal control theory*. Automation in Offshore Oil Field Operation. Proceedings of the IFAC/IFIP Symposium. Bergen, Norway. Vol.3, 183-188

Marintek. (2012b). SIMO – *User's Manual Version 4.0 rev. 1*. Norwegian Marine Technology Research Institute. Trondheim, Norway

American Bureau of Shipping. (den 1 May 2015). *ABS Record : ABS*. Retrieved from URL: http://www.eagle.org/safenet/record/record_vesseldetailsprinparticular?ReferrerApplication=PUBLIC

DNV GL AS. (29 April 2015). *SESAM DEEPC - MODULES*. Retrieved from URL: https://www.dnvgl.com/services/sesam-deepc-modules-2310

Floatel International AB. (2014). *Floatel Reliance Data Sheet.* Mölndal: Floatel International AB.

Floatel International Ltd. (22 April 2015). *Floatel International*. Retrieved from URL: www.floatel.se: http://www.floatel.se/Home__.html

Janson, C.-E. (2014). *Waves, Motions and Manoeuvring.* Chalmers University of Technology, Gothenburg

JCE Group of Companies. (2015, April 22). *The JCE Story*. Retrieved from URL: http://www.jcegroup.se/the_jce_story/consafe_offshore.aspx

MercoPress. (2012, Febuary 27). *Repsol-Sinopec makes huge oil discovery off-shore Brazil:250m boe*. Retrieved from URL: http://en.mercopress.com/2012/02/27/repsol-sinopec-makes-huge-oil-discovery-off-shore-brazil-250m-boe

Met Office UK. (2015, May 07ss). *Beafort wind force scale: Met Office*. Retrieved from URL: http://www.metoffice.gov.uk/guide/weather/marine/beaufort-scale

PETROBRAS. (den 1 May 2015). *Campos Basin: PETROBRAS SA*. Retrieved from URL: http://www.petrobras.com.br/en/our-activities/main-operations/basins/campos-basin.htm

Petrobras, Jurong Shipyard, & ForShip Engenharia Ltda. (2006). *ENVIRONMENTAL CONDITIONS AND MOTIONS.*

SBM Offshore. (den 1 May 2015). *Our Products, Turret mooring system: SBM Offshore*. Retrieved from URL: http://www.sbmoffshore.com/what-we-do/our-products/turret-mooring-systems/

Schiffahrtsinsttitut Warnemunde e.V. (den 12 May 2015). *Estimating potential danger of roll resonance for ship operation*. Retrieved from URL: http://schiw.sf.hs-wismar.de/siw/paper/heft5/beitrag10#12

Schreuder, M. (2014). *Developement, Implementation, Validation and Applications of a Method for Simulation of Damaged and Intact Ships in Waves.* Gothenburg: Chalmers University of Technology.

SOFEC. (2006). *Spread Moored or Turret Moored FPSO's for DEepwater Dield Developments.* Sofec.

wikiwaves. (den 11 May 2015). *Ocean Wave spectra: Wiki waves*. Retrieved from URL: http://www.wikiwaves.org/Ocean-Wave_Spectra

Appendix A – Thruster forces

Mean total thruster force for different orientations

Current 0.75 ms^{-1}							
Environmental Forces		Follow target			Station Keeping		
Direction	Characteristics H_s(m) /T_p(s) /V_w(ms^{-1})	Parallel Orientation	Diagonal Orientation	Perpendicular Orientation	Parallel Orientation	Diagonal Orientation	Perpendicular Orientation
22.5°	Case 2	285	490	572	287	678	547
	Case 3	332	571	667	331	721	630
	Case 4	460	735	886	471	855	824
45°	Case 2	285	461	549	278	605	481
	Case 3	339	535	636	342	624	561
	Case 4	453	683	834	493	712	717
90°	Case 2	208	340	440	301	422	1553[2]
	Case 3	329	402	483	153[1]	439	1872[2]
	Case 4	399	470	602	1704[2]	455	1614[2]

[1] Error in simulation after 2000 secs out of 10800 secs

[2] Simulation does not work

Case 2 = (2.5m/8s/10ms^{-1}) Case 3 = (3.5m/10s/12ms^{-1}) Case 4 = (4.5m/10s/15ms^{-1})

Current 1.0 ms^{-1}

Environmental Forces		Follow target			Station Keeping		
Direction	Characteristics H_s(m) /T_p(s) /V_w(ms^{-1})	Parallel Orientation	Diagonal Orientation	Perpendicular Orientation	Parallel Orientation	Diagonal Orientation	Perpendicular Orientation
22.5^o	Case 2	376	731	823	364	678	785
	Case 3	414	795	905	407	721	870
	Case 4	313	959	1124	550	855	1070
45^o	Case 2	390	705	808	346	605	712
	Case 3	435	761	881	410	624	797
	Case 4	560	901	1073	561	712	953
90^o	Case 2	313	576	682	317	442	576
	Case 3	375	594	690	374	439	618
	Case 4	493	662	822	529	455	682

Case 2 = (2.5m/8s/10ms^{-1}) Case 3 = (3.5m/10s/12ms^{-1}) Case 4 = (4.5m/10s/15ms^{-1})

12.1.1 Current 1.25 ms^{-1}

Environmental Forces		Follow target			Station Keeping		
Direction	Characteristics H_s(m) /T_p(s) /V_w(ms^{-1})	Parallel Orientation	Diagonal Orientation	Perpendicular Orientation	Parallel Orientation	Diagonal Orientation	Perpendicular Orientation
22.5^o	Case 1	376	931	971	371	895	954
	Case 2	681	1537	1669	462	973	1090
	Case 3	510	1086	1208	505	1016	1177
45^o	Case 1	684	905	979	1428[2]	1601[2]	1581[2]
	Case 2	479	989	1097	436	889	1010
	Case 3	538	1044	1183	503	903	1100
90^o	Case 1	351	846	919	1526[2]	747	1468[2]
	Case 2	429	885	1006	385	715	716
	Case 3	466	893	1041	481	700	910

Case 1 = (1.5m/6s/7ms^{-1}) Case 2 = (2.5m/8s/10ms^{-1}) Case 3 = (3.5m/10s/12ms^{-1})

Current 1.5 ms^{-1}							
Environmental Forces		Follow target			Station Keeping		
Direction	Characteristics H_s(m) /T_p(s) /V_w(ms^{-1})	Parallel Orientation	Diagonal Orientation	Perpendicular Orientation	Parallel Orientation	Diagonal Orientation	Perpendicular Orientation
22.5°	Case 1	496	1285	1337	490	1251	1320
	Case 2	597	1384	1488	584	1329	1460
	Case 3	644	1508	1883	626	1371	1550
45°	Case 1	482	1261	1336	294[1]	1633[2]	1287
	Case 2	590	1343	1453	551	1254	1376
	Case 3	654	1398	1552	614	1249	1470
90°	Case 1	450	1191	1267	1505[2]	1096	1202
	Case 2	551	1248	1535	529	715	1574
	Case 3	600	1266	1423	583	1038	1273

Case 1 = (1.5m/6s/7ms^{-1}) Case 2 = (2.5m/8s/10ms^{-1}) Case 3 = (3.5m/10s/12ms^{-1})

Appendix B – Correlation of Vessel and gangway0 motions

12.1.2 Parallel orientation/ Current: 1. 5ms^{-1} / Case 2 = (2.5m/8s/7ms-1)

12.1.2.1 Gangway stroke:

Table 7- 22.5^{o}

	Gangway stroke	Surge FPSO	Sway FPSO	Yaw FPSO
Gangway stroke		-0.397	-0.414	0.41
Surge Reliance	-0.50	0.68		
Sway Reliance	-0.2		0.96	
Yaw Reliance	0.507			0.92

Table 8-45^{o}

	Gangway stroke	Surge FPSO	Sway FPSO	Yaw FPSO
Gangway stroke		-0.414	-0.377	0.415
Surge Reliance	-0.508	0.7		
Sway Reliance	-0.283		0.89	
Yaw Reliance	0.5			0.92

Table 9- 90^{o}

	Gangway stroke	Surge FPSO	Sway FPSO	Yaw FPSO
Gangway stroke		-0.38	-0.37	0.37
Surge Reliance	-0.283	0.977		
Sway Reliance	-0.255		0.977	
Yaw Reliance	0.373			0.990

12.1.2.2 Gangway inclination:

Table 10-22.5º

	Gangway Inclination	Heave FPSO	Roll FPSO	Pitch FPSO
Gangway Inclination		-0.286	0.527	0.754
Heave Reliance	0.417	0.257		
Roll Reliance	-0.364		-0.15	
Pitch Reliance	0.402			0.18

Table 11-45º

	Gangway Inclination	Heave FPSO	Roll FPSO	Pitch FPSO
Gangway Inclination		0.336	-0.23	0.344
Heave Reliance	-0.376	0.28		
Roll Reliance	0.638		-0.21	
Pitch Reliance	0.710			0.187

Table 12-90º

	Gangway Inclination	Heave FPSO	Roll FPSO	Pitch FPSO
Gangway Inclination		0.22	-0.09	-0.25
Heave Reliance	-0.49	-0.20		
Roll Reliance	0.55		-0.41	
Pitch Reliance	0.54			0.22

12.1.3 Parallel orientation/ Current: 1. 25 ms-1 / Case 2 = (2.5m/8s/7ms-1)

12.1.3.1 Gangway stroke:

Table 13- 22.5°

	Gangway stroke	Surge FPSO	Sway FPSO	Yaw FPSO
Gangway stroke		-0.534	-0.531	-0.53
Surge Reliance	0.136	-0.357		
Sway Reliance	0.43		-0.468	
Yaw Reliance	0.369			0.117

Table 14-45°

	Gangway stroke	Surge FPSO	Sway FPSO	Yaw FPSO
Gangway stroke		0.123	0.122	0.122
Surge Reliance	-0.351	0.14243		
Sway Reliance	-0.18		0.201	
Yaw Reliance	0.40			-0.153

Table 15- 90°

	Gangway stroke	Surge FPSO	Sway FPSO	Yaw FPSO
Gangway stroke		0.126	0.125	0.125
Surge Reliance	-0.12	0.066		
Sway Reliance	-0.109		0.107	
Yaw Reliance	0.218			-0.040

12.1.3.2 Gangway inclination:

Table 16-22.5º

	Gangway Inclination	Heave FPSO	Roll FPSO	Pitch FPSO
Gangway Inclination		-0.042	-0.042	-0.042
Heave Reliance	-0.329	0		
Roll Reliance	-0.010		-0.04	
Pitch Reliance	-0.911			0

Table 17-45º

	Gangway Inclination	Heave FPSO	Roll FPSO	Pitch FPSO
Gangway Inclination		-0.009	-0.009	-0.009
Heave Reliance	-0.39	0.00		
Roll Reliance	0.60		-0.003	
Pitch Reliance	0.699			0.003

Table 18-90º

	Gangway Inclination	Heave FPSO	Roll FPSO	Pitch FPSO
Gangway Inclination		0.001	0.0012	0.0012
Heave Reliance	-0.45	0.00		
Roll Reliance	0.563		0.00	
Pitch Reliance	0.614			0.00

12.1.4 Parallel orientation/ Current: 1.0 ms-1 / Case 2 = (2.5m/8s/7ms-1)

12.1.4.1 Gangway stroke:

Table 19- 22.5°

	Gangway stroke	Surge FPSO	Sway FPSO	Yaw FPSO
Gangway stroke		-0.09	-0.09	-0.09
Surge Reliance	-0.43	0.136		
Sway Reliance	-0.27		0.202	
Yaw Reliance	0.411			-0.20

Table 20-45°

	Gangway stroke	Surge FPSO	Sway FPSO	Yaw FPSO
Gangway stroke		-0.035	-0.036	-0.035
Surge Reliance	-0.338	0.164		
Sway Reliance	-0.182		0.202	
Yaw Reliance	0.378			-0.18

Table 21- 90°

	Gangway stroke	Surge FPSO	Sway FPSO	Yaw FPSO
Gangway stroke		0.0681	0.067	0.0681
Surge Reliance	-0.0798	0.08		
Sway Reliance	-0.082		0.10	
Yaw Reliance	0.174			-0.073

12.1.4.2 *Gangway inclination:*

Table 22-22.5º

	Gangway Incl.	Heave FPSO	Roll FPSO	Pitch FPSO
Gangway Incl.		-0.018	-0.018	-0.018
Heave Reliance	-0.243	0		
Roll Reliance	0.471		-0.012	
Pitch Reliance	0.739			0.002

Table 23-45º

	Gangway Incl.	Heave FPSO	Roll FPSO	Pitch FPSO
Gangway Incl.		-0.021	-0.021	-0.021
Heave Reliance	-0.409	0.00		
Roll Reliance	0.561		-0.01	
Pitch Reliance	0.694			0.003

Table 24-90º

	Gangway Incl.	Heave FPSO	Roll FPSO	Pitch FPSO
Gangway Incl.		-0.002	-0.002	-0.002
Heave Reliance	-0.45	0.00		
Roll Reliance	0.56		0.000	
Pitch Reliance	0.61			0.00

12.1.5 Parallel orientation/ Current: 0. 75 ms-1 / Case 2 = (2.5m/8s/7ms-1)

12.1.5.1 Gangway stroke:

Table 25- 22.5º

	Gangway stroke	Surge FPSO	Sway FPSO	Yaw FPSO
Gangway stroke		-0.038	-0.039	-0.038
Surge Reliance	-0.354	0.143		
Sway Reliance	-0.176		0.205	
Yaw Reliance	0.315			-0.198

Table 26-45º

	Gangway stroke	Surge FPSO	Sway FPSO	Yaw FPSO
Gangway stroke		-0.009	-0.009	-0.009
Surge Reliance	-0.253	0.166		
Sway Reliance	-0.0980		0.20	
Yaw Reliance	0.290			-0.186

Table 27- 90º

	Gangway stroke	Surge FPSO	Sway FPSO	Yaw FPSO
Gangway stroke		0.051	0.050	0.0512
Surge Reliance	-0.0156	0.080		
Sway Reliance	-0.022		0.097	
Yaw Reliance	0.0998			-0.075

12.1.5.2 Gangway inclination:

Table 28-22.5º

	Gangway Incl.	Heave FPSO	Roll FPSO	Pitch FPSO
Gangway Incl.		-0.015	-0.015	-0.015
Heave Reliance	-0.237	0.00		
Roll Reliance	0.471		-0.0048	
Pitch Reliance	0.742			0.002

Table 29-45º

	Gangway Incl.	Heave FPSO	Roll FPSO	Pitch FPSO
Gangway Incl.		-0.019	-0.019	-0.019
Heave Reliance	-0.410	0.000		
Roll Reliance	0.564		-0.003	
Pitch Reliance	0.693			0.0029

Table 30-90º

	Gangway Incl.	Heave FPSO	Roll FPSO	Pitch FPSO
Gangway Incl.		-0.002	-0.0029	-0.002
Heave Reliance	-0.447	0.000		
Roll Reliance	0.585		0.0019	
Pitch Reliance	0.603			0.00

Appendix C – Relative motions of Vessels

Diagonal Orientation

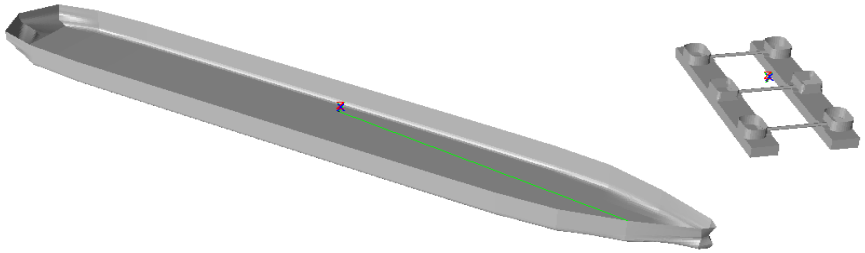

Current: 1.0 m/s **Case 3:** Hs= 3.5m Tp = 10s V=12ms^{-1} **Direction:** 22.5^{o}	**Current:** 1.5 m/s **Case 3:** Hs= 3.5m/Tp = 10s V=12ms^{-1}) **Direction:** 22.5^{o}
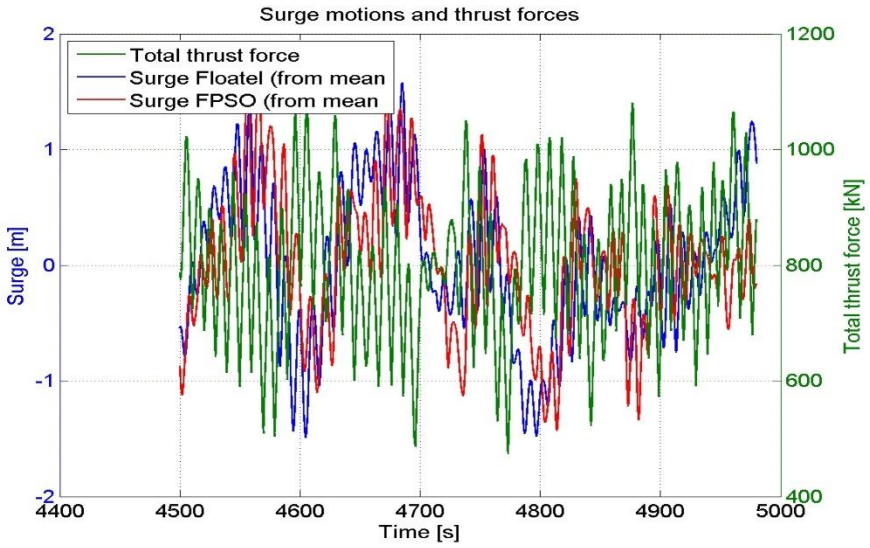	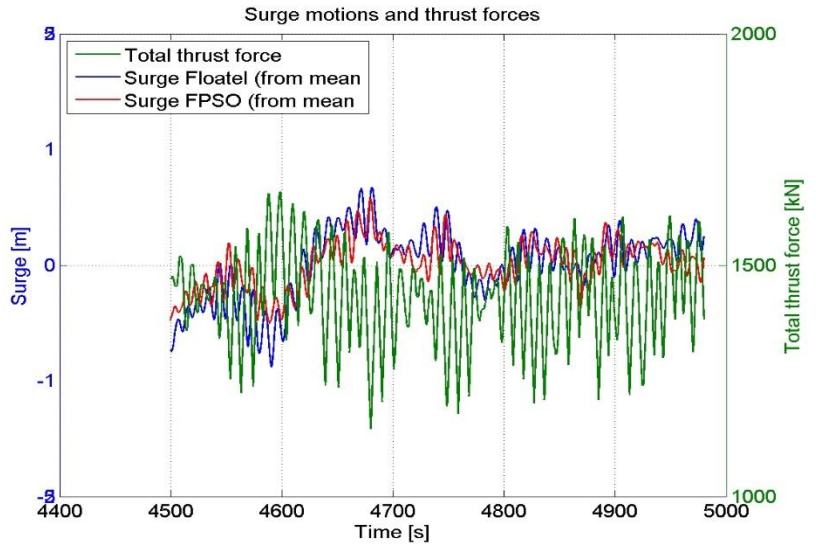

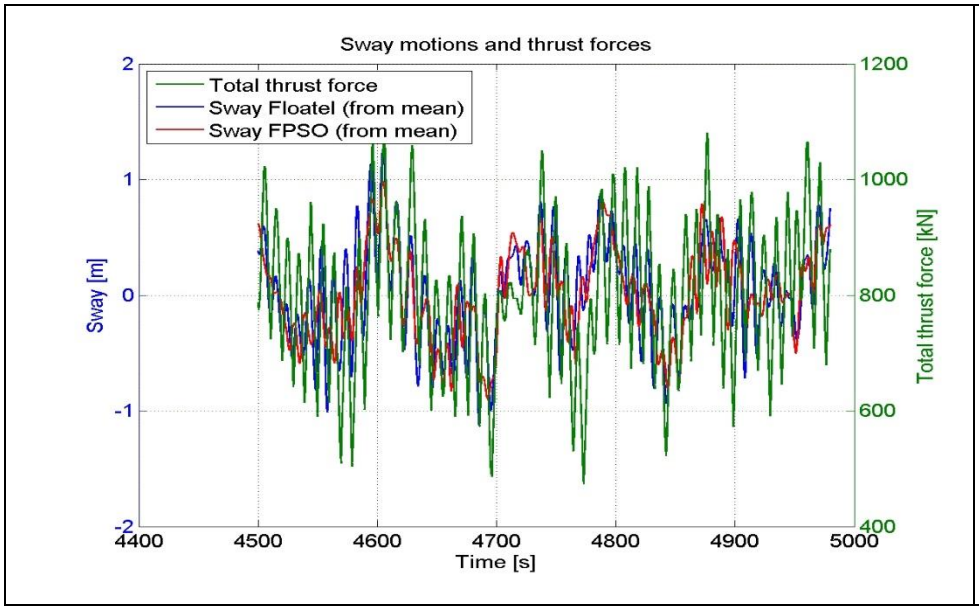
Sway motions and thrust forces
Total thrust force
Sway Floatel (from mean)
Sway FPSO (from mean)
Sway [m]
Total thrust force [kN]
Time [s]
2
1
0
-1
-2
1200
1000
800
600
400
4400
4500
4600
4700
4800
4900
5000

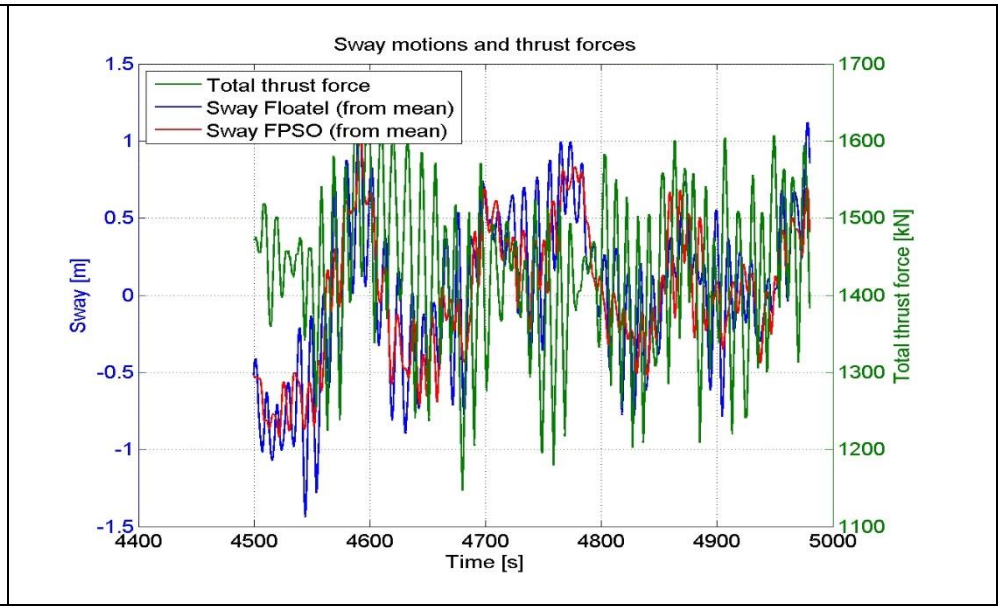
Sway motions and thrust forces
Total thrust force
Sway Floatel (from mean)
Sway FPSO (from mean)
Sway [m]
Total thrust force [kN]
Time [s]
1.5
1
0.5
0
-0.5
-1
-1.5
1700
1600
1500
1400
1300
1200
1100
4400
4500
4600
4700
4800
4900
5000

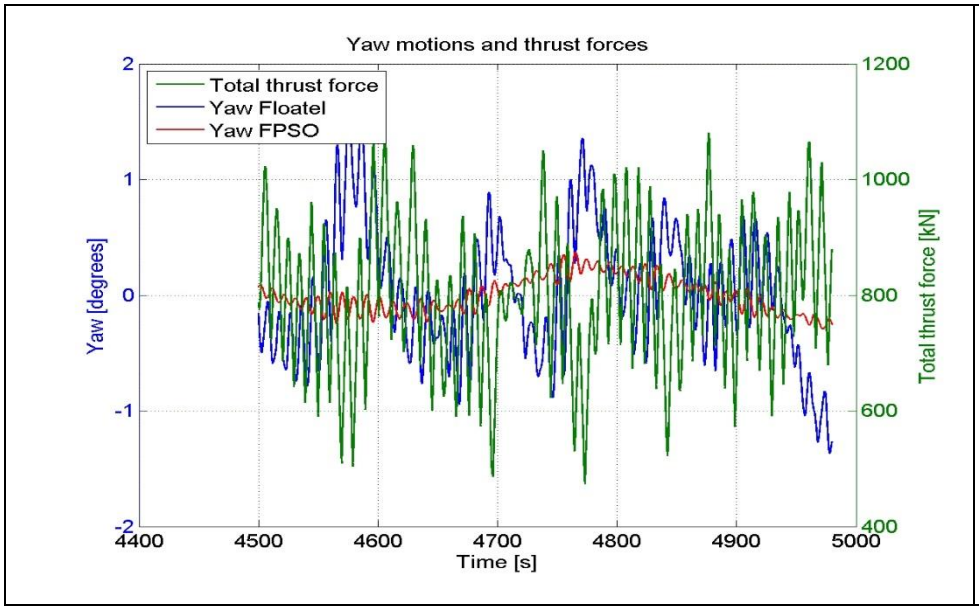
Yaw motions and thrust forces
Total thrust force
Yaw Floatel
Yaw FPSO
Yaw [degrees]
Total thrust force [kN]
Time [s]
2
1
0
-1
-2
1200
1000
800
600
400
4400
4500
4600
4700
4800
4900
5000

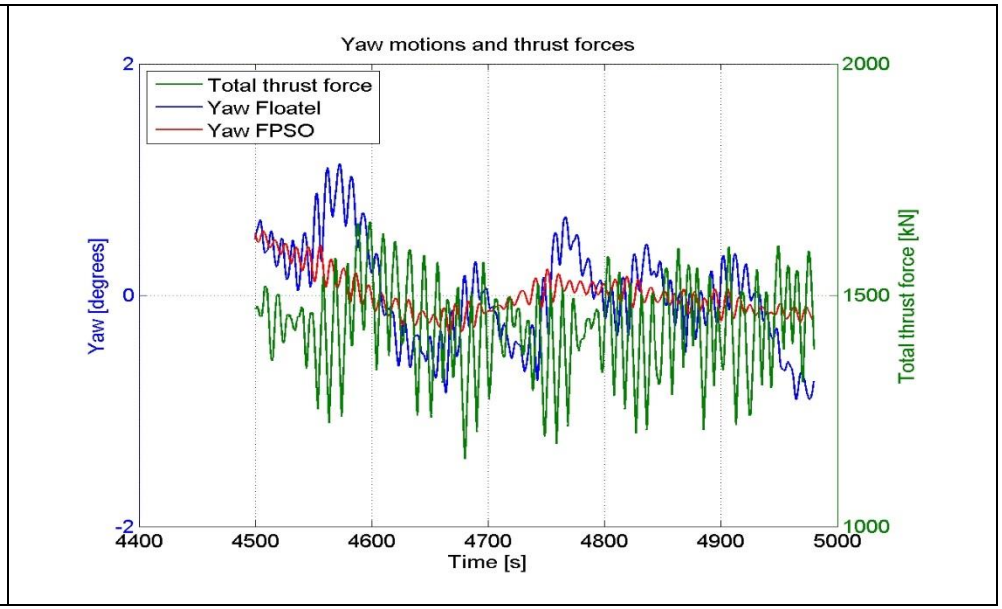
Yaw motions and thrust forces
Total thrust force
Yaw Floatel
Yaw FPSO
Yaw [degrees]
Total thrust force [kN]
Time [s]
2
0
-2
2000
1500
1000
4400
4500
4600
4700
4800
4900
5000

Parallel Orientation

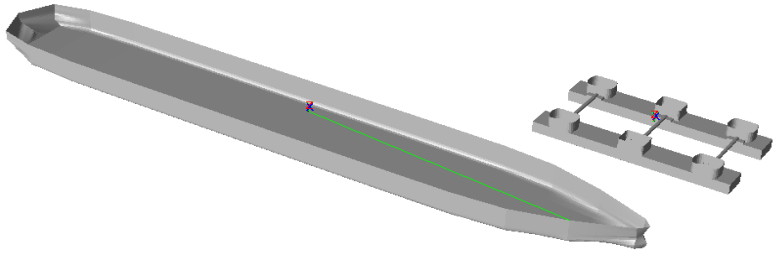

Current: 1.0 m/s **Case 3:** Hs= 3.5m/Tp = 10s V=12ms^{-1}) **Direction:** 22.5^{o}	**Current:** 1.5 m/s **Case 3:** Hs= 3.5m/Tp = 10s V=12ms^{-1}) **Direction:** 22.5^{o}
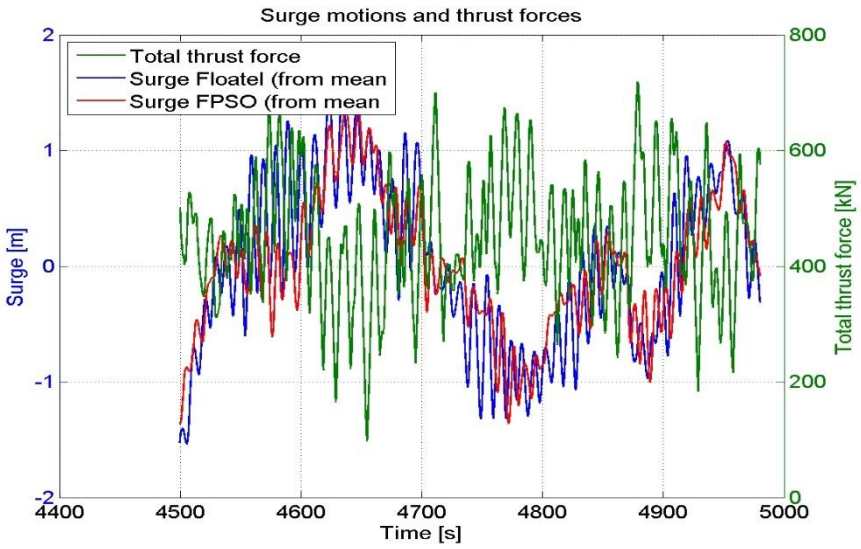	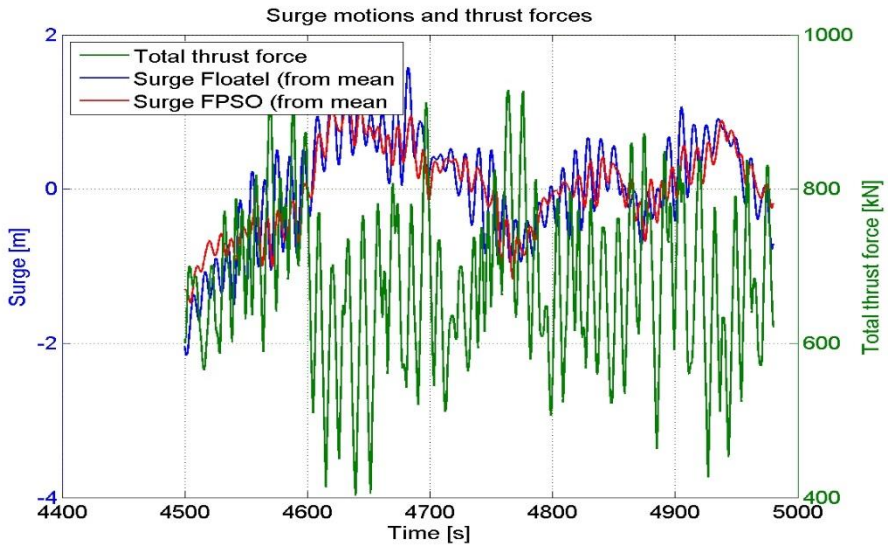

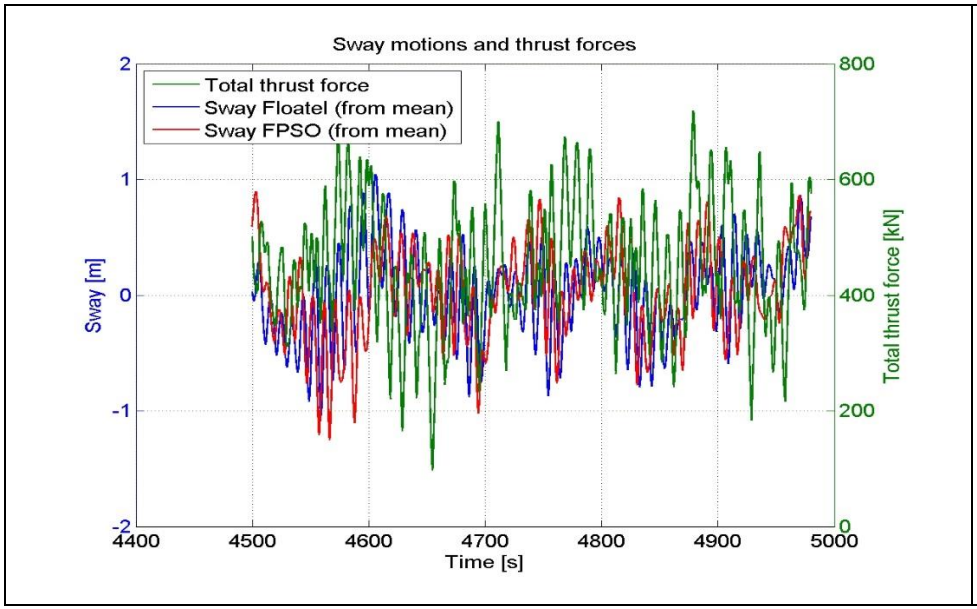
Sway motions and thrust forces
Total thrust force
Sway Floatel (from mean)
Sway FPSO (from mean)
Sway [m]
Total thrust force [kN]
Time [s]
2
1
0
-1
-2
800
600
400
200
0
4400
4500
4600
4700
4800
4900
5000

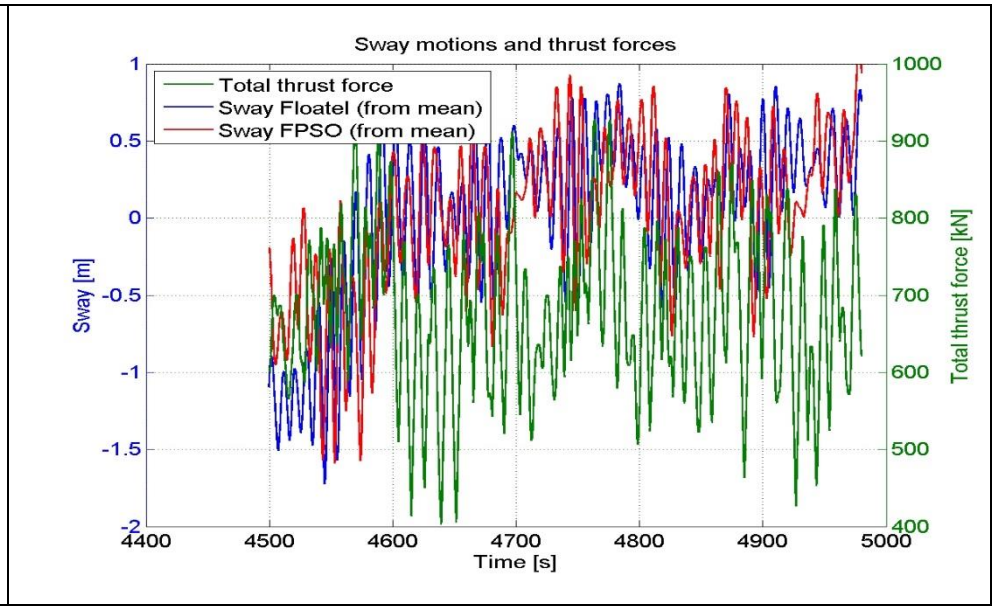
Sway motions and thrust forces
Total thrust force
Sway Floatel (from mean)
Sway FPSO (from mean)
Sway [m]
Total thrust force [kN]
Time [s]
1
0.5
0
-0.5
-1
-1.5
-2
1000
900
800
700
600
500
400
4400
4500
4600
4700
4800
4900
5000

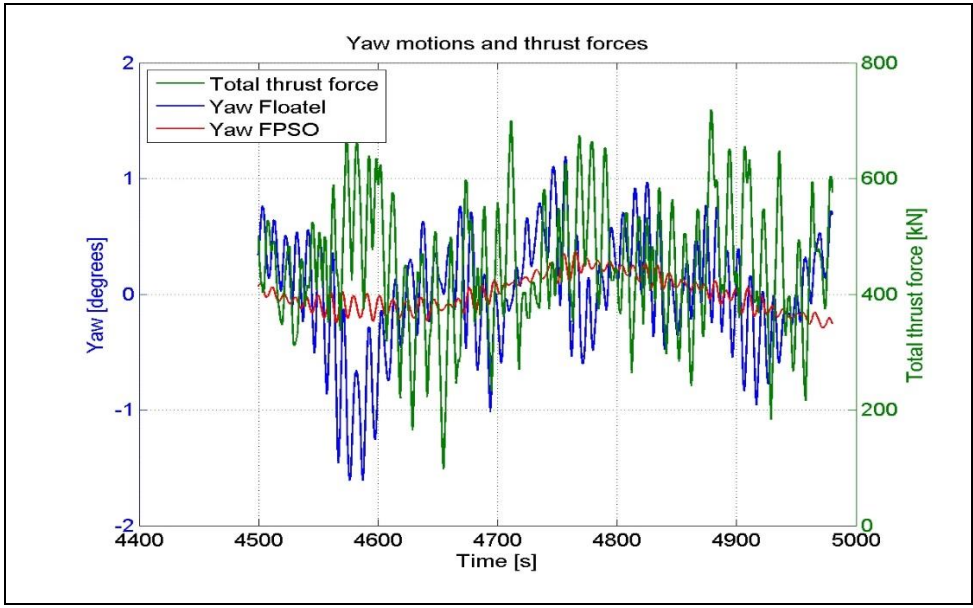

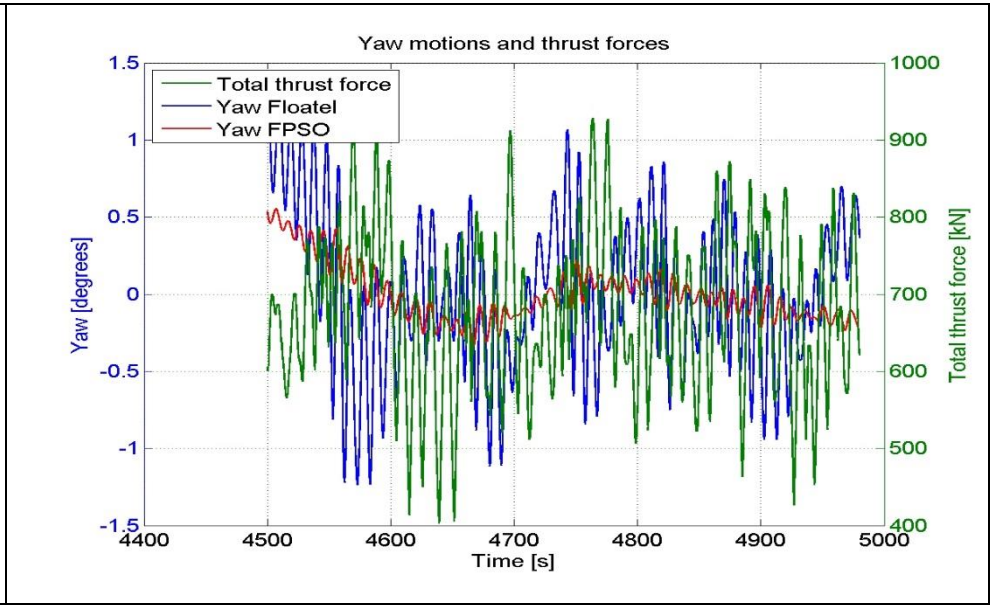

Perpendicular Orientation

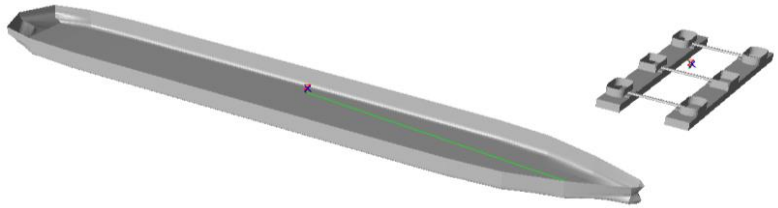

Current: 1.0 m/s **Case 3:** Hs= 3.5m/ Tp = 10s V=12ms^{-1}) **Direction:** 22.5^{o}	**Current:** 1.5 m/s **Case 3:** Hs= 3.5m/ Tp = 10s V=12ms^{-1}) **Direction:** 22.5^{o}

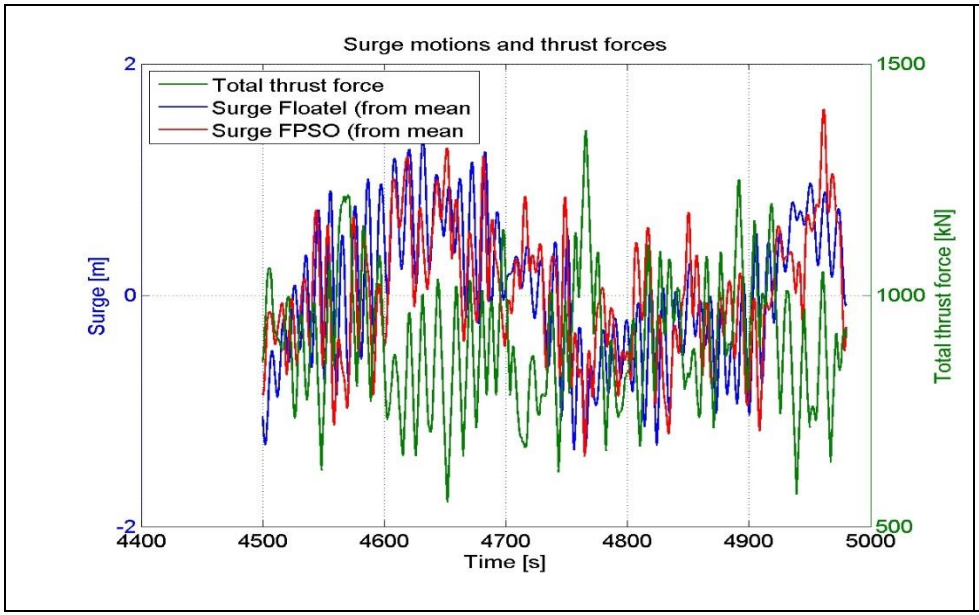
Surge motions and thrust forces
Total thrust force
Surge Floatel (from mean
Surge FPSO (from mean
Surge [m]
Total thrust force [kN]
Time [s]
2
0
-2
1500
1000
500
4400
4500
4600
4700
4800
4900
5000

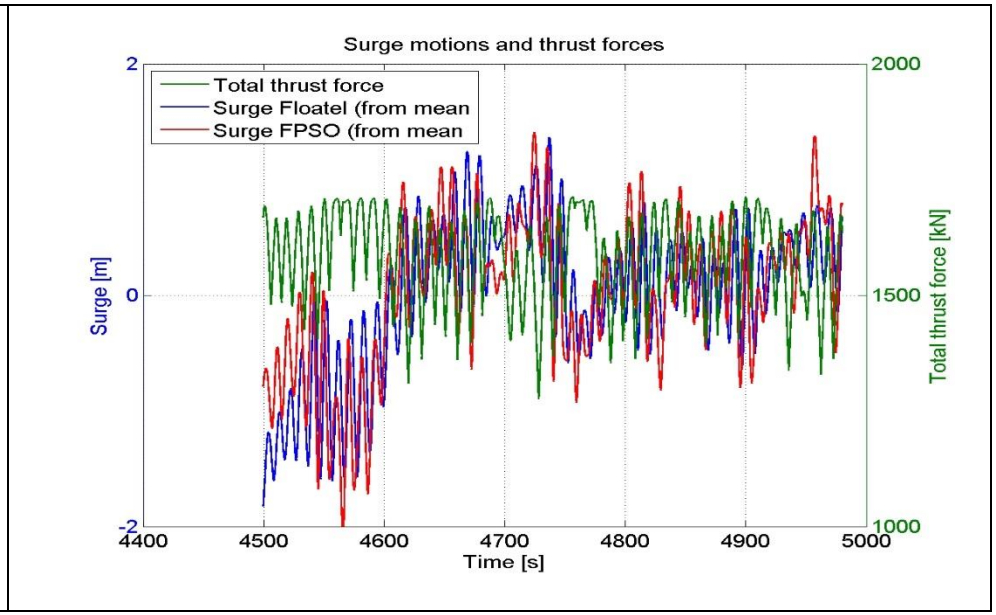
Surge motions and thrust forces
Total thrust force
Surge Floatel (from mean
Surge FPSO (from mean
Surge [m]
Total thrust force [kN]
Time [s]
2
0
-2
2000
1500
1000
4400
4500
4600
4700
4800
4900
5000

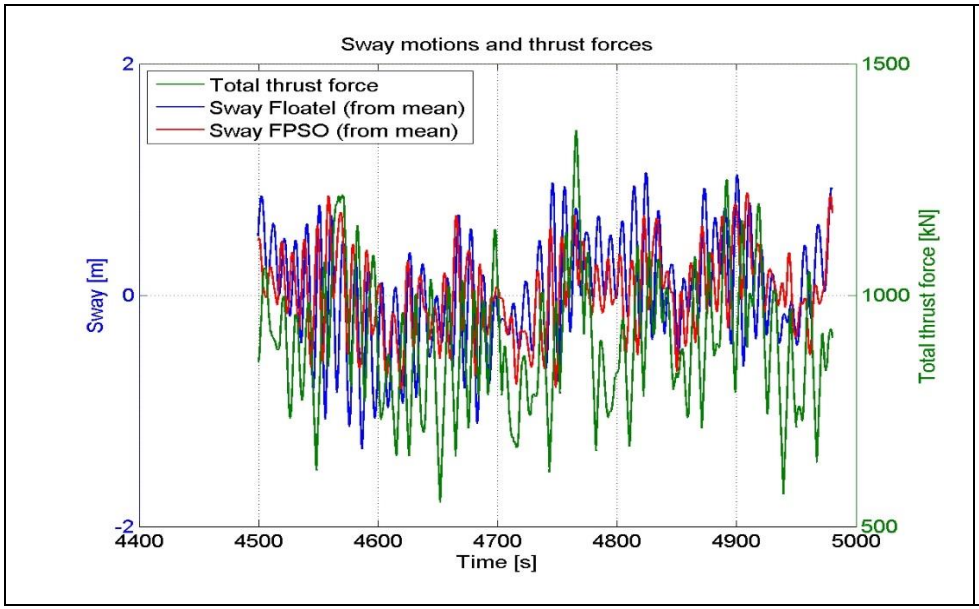
Sway motions and thrust forces
Total thrust force
Sway Floatel (from mean)
Sway FPSO (from mean)
Sway [m]
Total thrust force [kN]
Time [s]
2
0
-2
1500
1000
500
4400
4500
4600
4700
4800
4900
5000

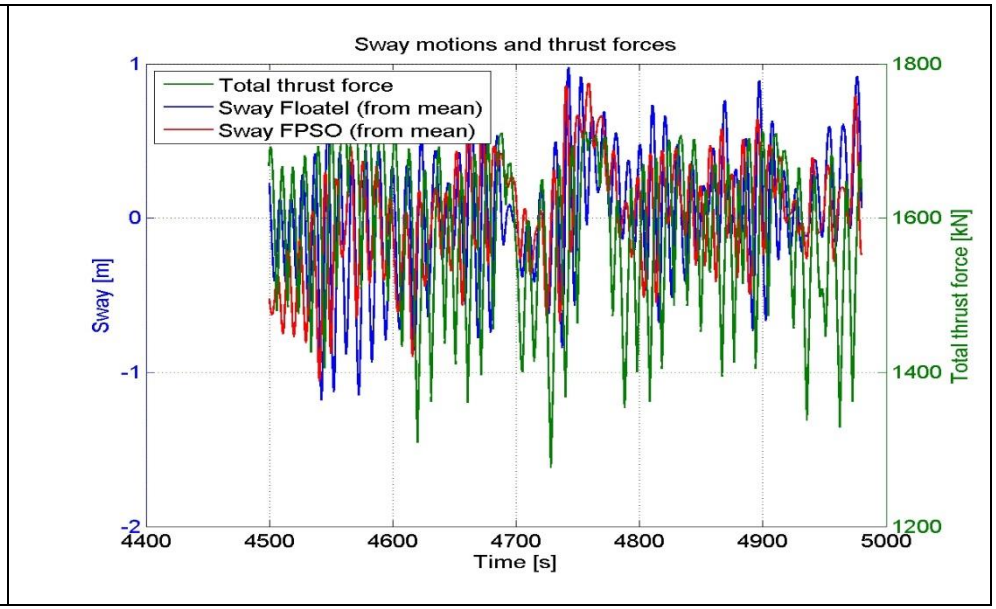
Sway motions and thrust forces
Total thrust force
Sway Floatel (from mean)
Sway FPSO (from mean)
Sway [m]
Total thrust force [kN]
Time [s]
1
0
-1
-2
1800
1600
1400
1200
4400
4500
4600
4700
4800
4900
5000

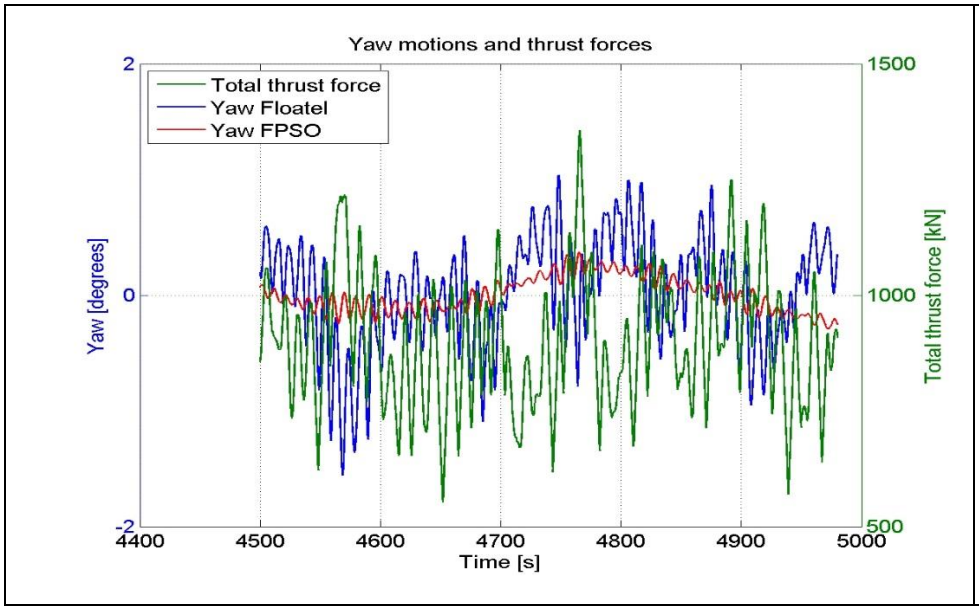
Yaw motions and thrust forces
Total thrust force
Yaw Floatel
Yaw FPSO
Yaw [degrees]
Total thrust force [kN]
Time [s]
2
0
-2
1500
1000
500
4400
4500
4600
4700
4800
4900
5000

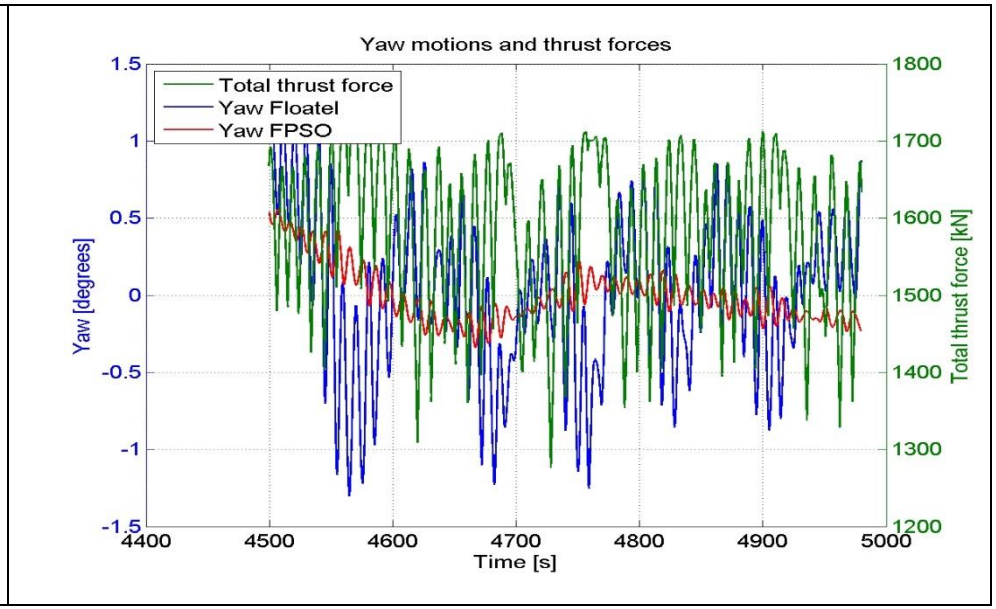
Yaw motions and thrust forces
Total thrust force
Yaw Floatel
Yaw FPSO
Yaw [degrees]
Total thrust force [kN]
Time [s]
1.5
1
0.5
0
-0.5
-1
-1.5
1800
1700
1600
1500
1400
1300
1200
4400
4500
4600
4700
4800
4900
5000